

Copyright © by

EDWIN JOHN HAMILTON, JR.

1969

- I. FREE RADICAL REACTION RATES BY
ELECTRON PARAMAGNETIC RESONANCE

- II. TERMINATION RATES OF SUBSTITUTED BENZO-
PHENONE KETYL RADICALS IN ALKANES

Thesis by

Edwin John Hamilton, Jr.

In Partial Fulfillment of the Requirements

For the Degree of

Doctor of Philosophy

California Institute of Technology

Pasadena, California

1970

(Submitted October 20, 1969)

ACKNOWLEDGEMENTS

To Professor George S. Hammond I express my great appreciation for his guidance, enthusiasm, and patience during the course of my graduate studies. It has been both highly instructive and enjoyable to be associated with him.

Much has also been learned from many of the graduate students and postdoctoral fellows in the Chemistry Department, especially those in the Hammond group. Indeed, interaction with these intelligent and intellectually curious people has been an outstanding feature of graduate study at Caltech.

I gratefully acknowledge the contribution to this work of Dr. David E. Wood who, in 1965, built the original version of much of the apparatus described in Part I of this Thesis. Thanks are also due to Mr. Carl C. Wamser who provided instruction and aid in operating the flash photolysis apparatus.

The competence and cordiality of the staff of the Chemistry Department are gratefully noted; particular thanks go to the men in the Instrument Shop.

The expert typing of this manuscript by Mrs. Eileen McKoy is gratefully acknowledged.

The California Institute of Technology is thanked for tuition scholarships and graduate teaching and research assistantships. The Petroleum Research Fund, administered by the American Chemical Society, is thanked for a fellowship.

ABSTRACT

PART I

A general method for the measurement of absolute rate constants for the termination of photochemically produced organic free radicals in solution has been developed. Radicals are generated in the cavity of an EPR spectrometer by high intensity UV irradiation of a suitable sample; an EPR spectrum is obtained from the steady-state concentration of intermediate radicals. The (second-order) decay of the EPR signal with time is followed after irradiation is abruptly stopped by mechanical means. Many such decay curves are averaged by computer. From the averaged decay curve plus a measurement of the steady-state radical concentration (by electronic double integration), absolute rate constants for radical termination are obtained. Rate constants as fast as diffusion-controlled may be determined by this technique.

PART II

Using the flash photolysis technique, the self-termination rate constants of benzophenone ketyl, 4,4'-dichlorobenzophenone ketyl, and 4,4'-dimethoxybenzophenone ketyl radicals were measured in a series of eight alkanes. These rate constants were all at least about 0.5 times, but clearly less than, the corresponding theoretical diffusion-controlled rate constants. Rate variations with solvent were satisfactorily accounted for by the theory of the effect of diffusion coefficient on an observed bimolecular rate constant. There was no significant rate variation with ketyl radical. Thus, the widely different

self-termination rate constants of the above ketyl radicals that have been measured in other solvents are due to substituent-dependent solvent effects. In benzene, these substituent effects may be due to charge-transfer complexing between radical and solvent.

TABLE OF CONTENTS

	<u>PAGE</u>
PART I	
INTRODUCTION	2
OPTICAL SYSTEM	8
ROTATING SECTOR	10
ELECTRONIC DOUBLE INTEGRATOR	11
SAMPLES	18
DISCUSSION	24
REFERENCES	28
PART II	
INTRODUCTION	33
Chemical Aspects	35
Diffusional Aspects	38
EXPERIMENTAL	44
Ketones	44
Alkanes	44
Sample Preparation	45
Flash Photolysis - Kinetic Spectrophotometry	45
Flash Photolysis - Flash Spectroscopy	46
RESULTS	46
Ultraviolet Absorption Spectra of Ketones	46
Flash Photolysis - Spectra	48
Flash Photolysis - Kinetics	51

	<u>PAGE</u>
DISCUSSION	58
Noyes Equation	58
Interpretation of Data	61
Conclusions	80
REFERENCES	81
PROPOSITIONS	85

LIST OF FIGURES

PART I

FIGURE	TITLE	PAGE
1	Schematic Side View of the Optical System	9
2	Schematic of Electromechanical Apparatus for Generating Trigger Signal for the CAT	12
3	Schematic Circuit of Electronic Single Integrator	13
4	An Example of Data Output from the CAT Memory	25

PART II

FIGURE	TITLE	PAGE
1	Ultraviolet Absorption Spectra of Substituted Benzophenones	47
2	An Example of Flash Photolysis Kinetic Data	53
3	A Plot of k as a Function of D_{12}^0	59
4	A Plot of k_D as a Function of D_{12}^0	60
5	A Plot of α as a Function of D_{12}^0	62
6	A Plot of $1/\alpha - 1$ as a Function of D_{12}^0	63
7	A Plot of Decay Data for Benzophenone Ketyl Radical in Several Alkanes	72
8	A Plot of Decay Data for 4, 4' -Dichloro- benzophenone Ketyl Radical in Several Alkanes	73
9	A Plot of Decay Data for 4, 4' -Dimethoxy- benzophenone Ketyl Radical in Several Alkanes	74

LIST OF TABLES

PART II

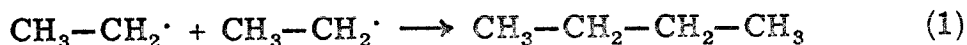
TABLE	TITLE	PAGE
1	Solution Concentrations and Monitoring Wavelengths	51
2	Experimental Values of k_{obs}/ϵ for the Bimolecular Decay of Ketyl Radicals	56
3	Viscosities, Le Bas Molar Volumes, and Estimated Molecular "Diameters" of Solvents	64
4	Calculated Ketyl Radical Parameters	66
5	Calculated Diffusion-Dependent Quantities for the Self-Termination of Benzophenone Ketyl Radicals	67
6	Calculated Diffusion-Dependent Quantities for the Self-Termination of 4, 4'-Dichlorobenzophenone Ketyl Radicals	68
7	Calculated Diffusion-Dependent Quantities for the Self-Termination of 4, 4'-Dimethoxybenzophenone Ketyl Radicals	69
8	Least Square Parameters and Standard Errors for the Fit of Points to the Noyes Equation	75
9	Values of ϵ and k_c and Their Standard Errors	76
10	Values of k_{obs} for the Bimolecular Decay of Ketyl Radicals	77
11	Rate Constants for Ketyl Radical Termination in Benzene	79

PART I

FREE RADICAL REACTION RATES BY
ELECTRON PARAMAGNETIC RESONANCE

INTRODUCTION

A characteristic property of most free radicals is reaction together in pairs to produce a diamagnetic molecule or molecules. Such reactions are called termination reactions and are of two types: coupling and disproportionation. In the case (1) of ethyl radicals, for instance, coupling produces n-butane



while disproportionation involves a hydrogen atom transfer and produces one ethane and one ethylene molecule:



For radicals larger than ethyl, these termination reactions always follow second-order rate laws (2), that is

$$-\frac{d[\text{R}\cdot]}{dt} = 2k[\text{R}\cdot]^2 \quad (3)$$

where $[\text{R}\cdot]$ is the free radical concentration, and k is the bimolecular rate constant. In fluid solution, values of k for most monomeric radicals are very large and approach diffusion-controlled rate constants of 10^9 - $10^{10} \text{ M}^{-1} \text{ sec}^{-1}$.

Because these termination reactions are usually so fast, the absolute rate constants are not easily measured. Thus, prior to the development of the experimental technique which will be described in

the first part of this thesis, only a few such rate constants had been measured. One method used in these earlier studies is the rotating sector technique (3). In cases when the rather restrictive kinetic requirement (that the rate of formation of a product during steady illumination be proportional to the light intensity to a power other than zero or one) is fulfilled, this technique has been used (4) to determine absolute bimolecular rate constants up to nearly diffusion-controlled. A second method which has been used is flash photolysis. In the application of this technique (5), a powerful and very short flash of light produces a significant concentration of intermediate free radicals; kinetic optical spectrophotometry is employed to directly observe the decay of the radical concentration after the flash. In order to obtain the bimolecular decay rate constant, it is also necessary to determine the extinction coefficient of the radical at the monitoring wavelength. In a method otherwise similar to flash photolysis, a pulsed beam of electrons from a linear accelerator has been used for radical generation (6).

Electron paramagnetic resonance (EPR) is uniquely suited to the study of free radical reactions because of its selectivity to species with unpaired electrons. Thus, interfering absorption by nonradical species in the sample can be a problem in the flash photolysis technique but cannot occur at all if EPR is used as the radical detector. Another advantage is that in EPR absorption the "extinction coefficients" of all radicals are equal and therefore need not be separately measured, contrary to the case with absorption of

optical radiation. The complex kinetics necessary in the rotating sector technique are, of course, not required if the radical intermediates are directly observed by any technique.

By continuous irradiation of a sample in an EPR cavity with an electron beam, Fessenden and Schuler produced a sufficient steady-state concentration of free radicals to study their EPR spectra (7). Pulse radiolysis with an electron beam permits direct observation of radical formation and decay by monitoring the EPR signal; from an averaged decay curve plus a measurement of either steady-state radical concentration or rate of radical formation, bimolecular rate constants have been determined (8, 9). As a possible alternative to obtaining an averaged decay curve, Fessenden has shown that, by direct analogy with the rotating sector technique, the average radical lifetime can be determined by measuring EPR signal height as a function of pulse rate (8).

Recently, flash photolytic generation of free radicals has been combined with EPR detection. Using a sampling technique similar to that of Ingram and co-workers (10, 11), Bennett, Smith, and Wilmschurst (12, 13) have measured the bimolecular decay rate constant for benzophenone radical anion ($k \sim 10^6 \text{ M}^{-1} \text{ sec}^{-1}$). Their method is the following: after a 100 μsec intense flash, the decaying EPR signal is sampled at several discrete times; the flashes are repeated every 1.5 sec, and the magnetic field of the spectrometer is swept slowly through the resonance. Thus, several complete EPR spectra are obtained, each corresponding to a fixed time after the

flash. From points of equal magnetic field on the several spectra, radical decay curves may be constructed. A similar technique has been described by Atkins, McLauchlan, and Simpson (14). After a 1 msec half-width intense flash, the decaying EPR signal is monitored by a computer of average transients (CAT); with the magnetic field held constant, the flashes are repeated many times until an averaged decay curve of sufficient signal/noise ratio is achieved. The magnetic field is varied incrementally and many averaged decay curves are recorded, from which EPR spectra corresponding to hundreds of times after the flash may be constructed. The decay of benzophenone radical anion was studied by these workers also. It appears that recent techniques of extremely rapid magnetic field sweep (15, 16) coupled with flash photolysis may be an alternative to the two methods just described.

A new experimental method for the measurement of absolute rate constants for the termination of photochemically produced free radicals in solution has been developed in this laboratory. Study of the EPR spectra of short-lived organic free radicals in solution by continuous UV irradiation of a suitable sample inside the resonant cavity of an EPR spectrometer is a well-established technique (17-32). This technique has been extended to permit direct observation of the free-radical concentration as a function of time after irradiation of the sample is abruptly stopped.

Basically, this new method involves monitoring the decay of the EPR signal of a free-radical intermediate when the reaction-

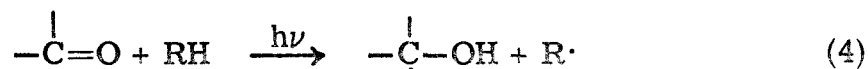
initiating light is mechanically blocked; since any one decay signal is, in general, completely obscured by noise, many such decays are averaged by a CAT until an adequate signal/noise ratio is achieved. From this averaged curve, plus a measurement of the steady-state radical concentration ($[R\cdot]_{SS}$), rate constants can be calculated.

The components of the apparatus are a Varian V-4502-12 EPR Spectrometer with V-4532 Dual Sample Cavity and G-22A Dual Channel Recorder, a Fabri-Tek Model 1062 Instrument Computer with SD-3 and SW-7 plug-in units, an electronic double integrator, a Hanovia 2500 watt Xenon-Mercury D. C. Lamp with starter and power supply, an optical system, and a rotating sector. Some of these components will be described further in succeeding sections.

Using this technique (33), workers in this laboratory have measured the bimolecular decay rates of many radicals of several types. The radicals studied include hydrocarbon radicals from the photolysis of azo compounds (34), t-butoxy radical from the photolysis of t-butyl peroxide (35), ketyl radicals from the photoreduction of ketones (36), α -keto ketyl radicals from the photoreduction of α -diketones (37), ketyl-type radicals from the photoreduction of α -keto acids and esters (38), and semiquinone radicals from the photoreduction of quinones (39).

The applicability of this technique in the determination of decay rate constants of many other radicals is indicated by several recent studies in the literature. In these studies, a steady-state concentration of free radicals, which probably terminate at close to

the diffusion-controlled rate, was produced in the cavity of an EPR spectrometer by continuous UV irradiation of a suitable fluid solution sample; this steady-state concentration was generally high enough for high resolution EPR spectra to be obtained. For instance, photoreduction of carbonyl compounds according to the equation



where RH is a hydrogen donor, has permitted EPR observation of ketyl free radicals, and sometimes also of R· (18, 20, 25-27). Similarly, EPR spectra of α -keto ketyl and R· radicals have been obtained by photoreduction of α -diketones (20). Semiquinone radicals have been observed by photoreduction of quinones (22-24, 26). Photolysis of H₂O₂ in alcohols has resulted in EPR spectra of α -hydroxy (17) and β -hydroxy (19) carbon radicals. Radicals derived from amides and an imide have been obtained by hydrogen abstraction from the parent compounds, either by HO· from the photolysis of H₂O₂ or by an excited state of acetone (21). In what appears to be an excellent and general technique, Krusic, Kochi, and co-workers (28-32) have studied the EPR spectra of a large variety of hydrocarbon radicals generated by selective hydrogen abstraction from the parent hydrocarbons by t-butoxy radical; this latter radical is itself generated by photolysis of t-butyl peroxide.

A comparison of our technique for the measurement of bimolecular radical decay rate constants with the other methods described earlier is useful. The virtue of EPR detection in the study of

free radical reactions has already been mentioned. For the generation of free radicals, high power UV lamps are much more available than are electron beam sources; in addition, optical radiation generally permits a far greater degree of selectivity in radical generation than does electron beam irradiation. At present, the two flash photolysis-EPR techniques are inferior to the continuous irradiation with mechanical interruption method described here. This is due to the fact that the product (flash energy \times flash frequency) for the former techniques is very much less than the lamp intensity for the latter technique. Therefore the average radical concentration is also much smaller. For instance, the high resolution study of benzophenone radical anion by Atkins *et al.* (14c) took 60-78 hrs; using the method described here, the time would be a few minutes. Thus, the comparison of techniques by Bennett *et al.* (13) on the basis of equality of the above product with a continuously operated lamp's intensity is not relevant at present.

A description of various components of our apparatus and a discussion of some operational considerations follows.

OPTICAL SYSTEM

The optical system is shown schematically in Fig. 1. The essential feature of these optics is twice focusing the light beam to a small spot--first, at the rotating sector, and second, at the entrance hole of the microwave cavity. It is desirable to have the cross section of the light beam as small as possible at the rotating sector in

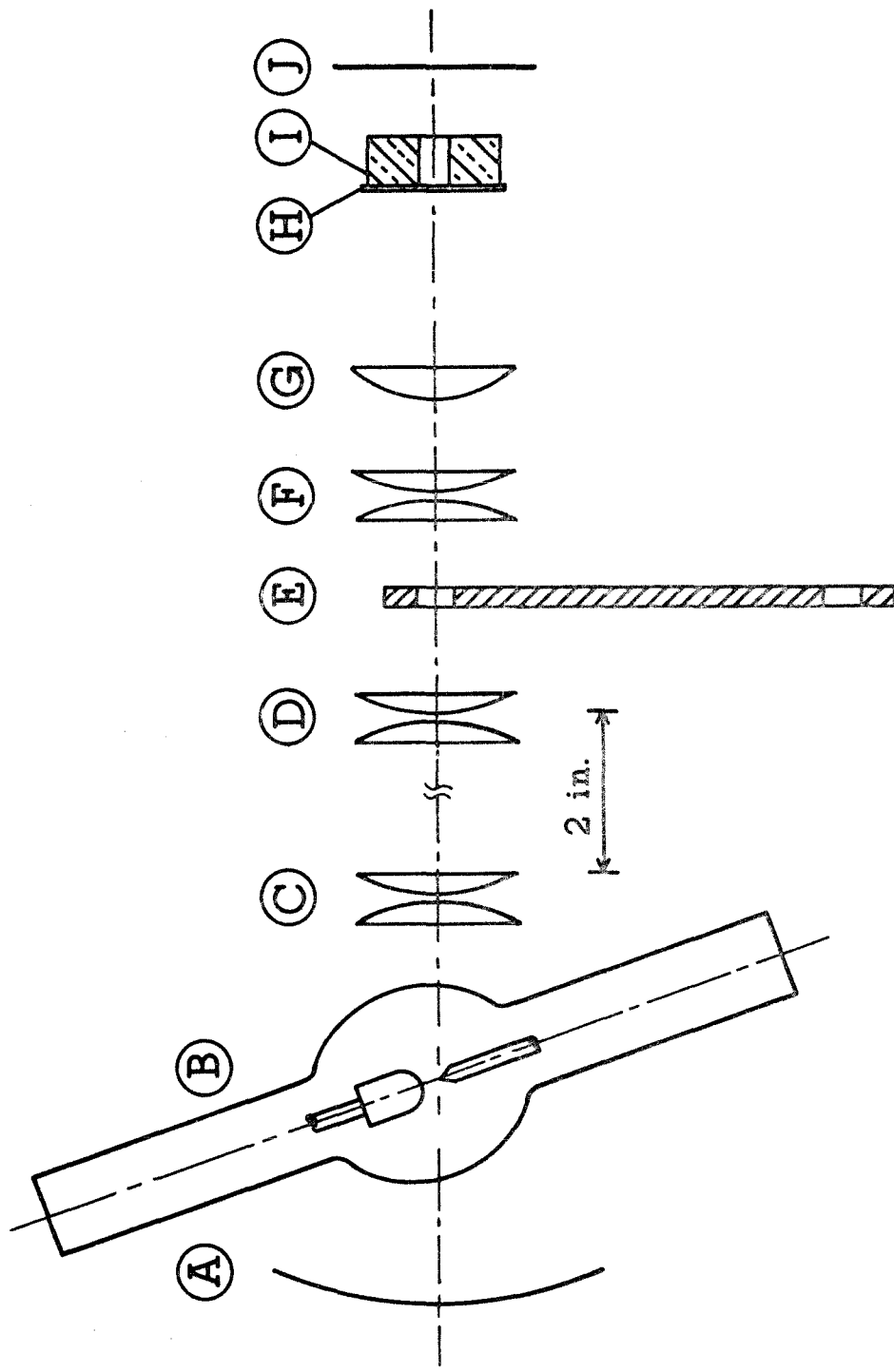


Figure 1. Schematic side view of the optical system. A, spherical mirror of 10 cm focal length; B, 2.5 kw lamp; C, D, F, compound lenses of about 5 cm focal length; each is made up of two nearly touching quartz lenses of 10 cm focal length; E, rotating sector; G, quartz lens of 7.5 cm focal length; H, 1.6 mm thick quartz plate; I, copper front plate of microwave cavity; J, sample center line. A water-cooled filter solution holder is positioned between C and D but is not shown.

order to minimize the time that the leading edge of the sector is passing across the width of the beam, during which period the chemical kinetics are hopelessly complex. The purpose of the quartz plate, H, at the cavity entrance is to eliminate the "wind effect" of the rotating sector which increases spectrometer noise. The 50% transmission slotted plate which is standard on the Varian V-4532 cavity was replaced with the copper plate, I, which is 15.9 mm thick and has a 9.5 mm diameter hole in the center; this change permits 100% transmission of an incident beam and causes no loss of spectrometer sensitivity.

The sensitive region of a sample tube in an EPR cavity is, in general, of rectangular cross section; therefore, an optimum optical system for in situ irradiation would presumably have a light beam of elliptical cross section entering the cavity, obtainable through the use of a cylindrical lens(es). Since the Varian slotted plate does provide a rectangular area for light transmission, it is relevant to mention that it was found possible to widen the slots in this plate to the point of 85% transmission, with a loss in sensitivity of only 10%.

ROTATING SECTOR

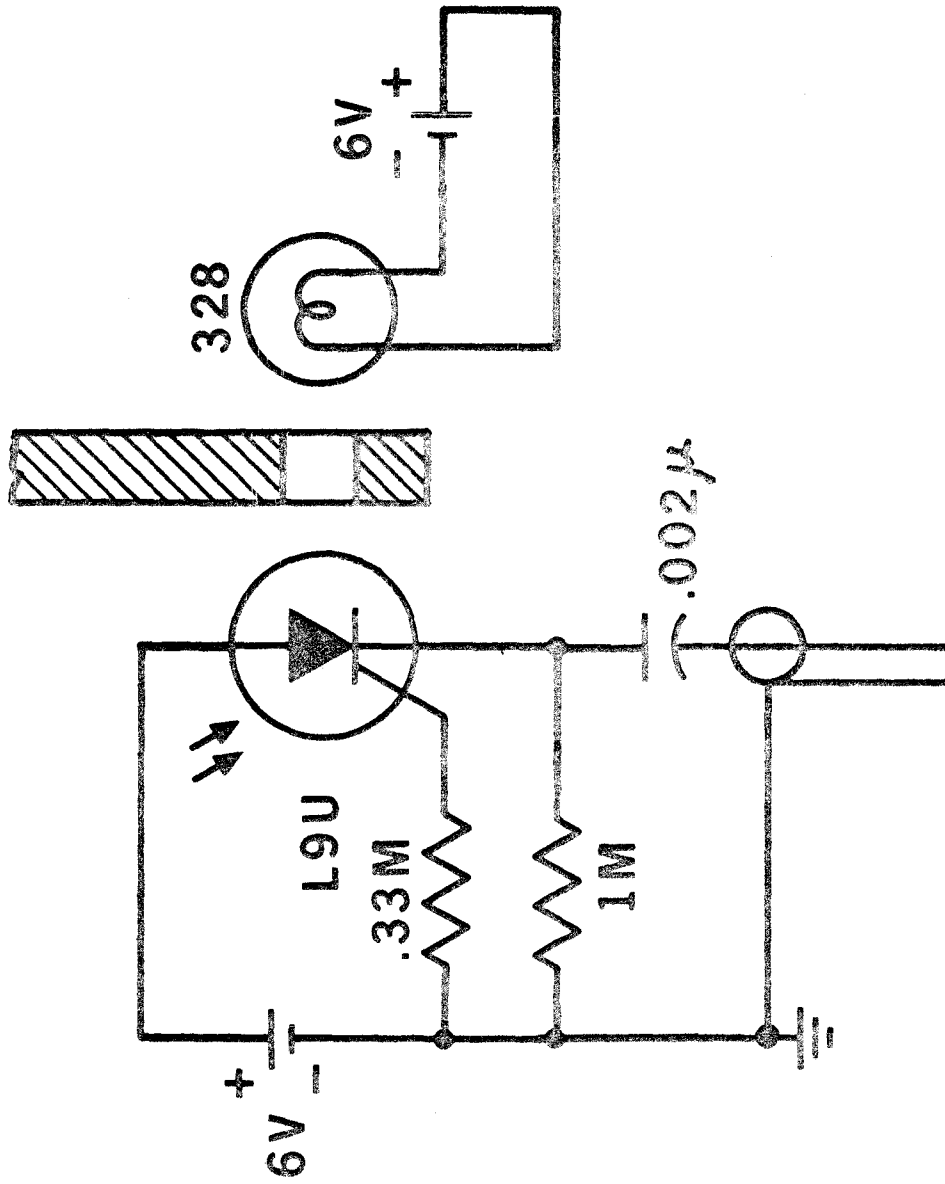
The rotating sector, E, is shown in Fig. 1, and is a circular disc with two opposed 90° annular sectors cut out; equal light and dark periods are thus provided. The sector is rotated by a Bodine NSE-11 motor with an SE-11 variable speed controller. This rotating disc is in a region of significant magnetic field and therefore cannot be a

conductor; furthermore, it must be strong because of the stresses of high speed; and it must be heat resistant because of the high intensity of the incident light beam. The material used is Epiall 1914 (Mesa Products), a moulded epoxy resin. It is desirable to use a guard over this rotating sector, since it once disintegrated during operation.

Mounted on the same shaft as the sector disc is a circular aluminum disc with two 3.2 mm holes near the edge, 180° apart. When one of these holes passes between a light bulb and a light-activated silicon-controlled rectifier (LASCR), as shown in Fig. 2, a voltage pulse is produced for triggering the CAT. The relative phase of the rotating sector and trigger disc is set so that a pulse occurs when the sector has just completely blocked the light beam.

ELECTRONIC DOUBLE INTEGRATOR

In EPR, as in other types of absorption spectroscopy, the integral of the absorption curve with respect to frequency is proportional to the number of absorbing species present. Since EPR spectra are the first derivatives of absorption curves, double integration of the spectra is necessary. An electronic double integrator, half of which is shown schematically in Fig. 3, has been built; it is essentially a highly simplified version of the analog computer described by Randolph (40). The amplifiers and power supply are Burr Brown Models 3010 and 501 respectively; the feedback capacitors are Electrocube polycarbonates. It was found necessary to use these very



TO CAT

Figure 2. Schematic side view of second rotating disc and electronics for generating synchronized trigger signal for the CAT.

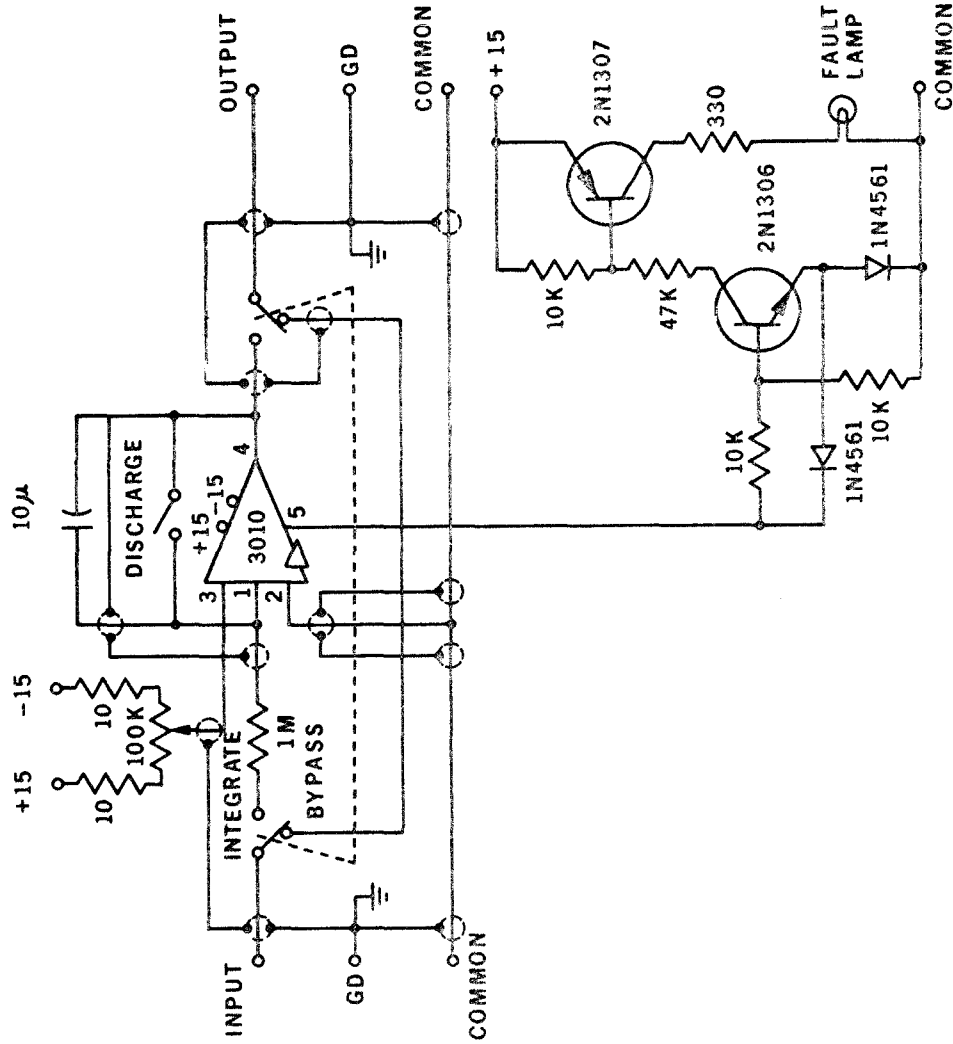


Figure 3. Schematic circuit of electronic single integrator; the double integrator described here is composed of two such single integrators in series.

low leakage capacitors in order to obtain the full theoretical output of the circuit. The equation giving the double integrator output signal (e_o) as a function of the input signal (e_i) is

$$e_o = - \frac{1}{T_2} \int \left(- \frac{1}{T_1} \int_0^t e_i dt' \right) dt \quad (5)$$

where T_1 and T_2 are the time constants (input resistance \times feedback capacitance) of single integrators 1 and 2 respectively. The internally generated drift of this double integrator was negligibly small for most cases. In any event, this drift can always be subtracted out since it was predictable by equation 5 from a knowledge of the individual single integrator linear drift rates (D_1 and D_2). The total drift of the double integrator during the time τ is then given by

$$D_2 \tau - \frac{D_1 \tau^2}{2T_2} \quad (6)$$

for integrator 1 preceding integrator 2. Since

$$D_j = \frac{a_j}{T_j} \quad (j = 1, 2) \quad (7)$$

where a_j is characteristic of the j th amplifier, the total drift can be written as

$$\frac{a_2 \tau}{T_2} - \frac{a_1 \tau^2}{2T_1 T_2} \quad (8)$$

An initial attempt to double integrate using one amplifier in an appropriate circuit was defeated by excessively high drift.

Two additional possible contributions to error in double integration of an EPR signal will be considered. If the base line output of the spectrometer is offset from zero by an amount b , then the contribution to the double integral will be

$$\frac{1}{T_1 T_2} \int_{t=0}^{\tau} \int_{t'=0}^t b dt' dt = \frac{b\tau^2}{2T_1 T_2} \quad . \quad (9)$$

If the spectrometer base line drifts linearly (drift = ct) as sometimes happens, the contribution to the double integral will be

$$\frac{1}{T_1 T_2} \int_{t=0}^{\tau} \int_{t'=0}^t ct dt' dt = \frac{c\tau^3}{6T_1 T_2} \quad . \quad (10)$$

Since the double integral of an EPR first derivative spectrum can be written as

$$\frac{d\tau^2}{T_1 T_2} \quad (11)$$

where d is a constant depending on the EPR signal, it is seen that the ratio of error due to base line offset (equation 9) to the real signal (equation 11) is independent of adjustable parameters; however, the ratio of base line drift error (equation 10) to signal (equation 11) is proportional to τ . Thus, if base line drift is bad enough, a short double integrating time is favored.

For an EPR first derivative spectrum to exhibit approximately the natural line shape, it is necessary that both the magnetic field modulation amplitude and the product (magnetic field scan rate \times detector time constant) be a small fraction of the line width. It is well known that the double integral of an EPR signal is linear in field modulation amplitude in the ranges of both natural and overmodulated line shapes (40). This result permits one to increase signal/noise ratio when double integrating by using higher field modulation amplitudes than can be used in a high resolution study. It has also been shown that the first moment of an EPR first derivative spectrum is independent of distortion of the latter by detector response (41). Since the double integral is the same as the first moment, it will also be independent of such distortion. This result is important because it permits double integration of an EPR signal in a time short enough to minimize error arising from drift in the spectrometer base line.

This result has been confirmed experimentally by numerical double integration of distorted (natural line width \approx detector response time) and undistorted (natural line width $\approx 10 \times$ response time) single line spectra of pitch in KCl. Within experimental error, the double integrals (expressed in units of gauss²) were equal. The double integrals were calculated using the equation

$$\text{double integral} = \frac{(\Delta X)^2}{2} \sum_{i=1}^n (n+1-2i)y_i \quad (12)$$

where ΔX is the increment of magnetic field, n is the number of increments into which the magnetic field interval of non-negligible EPR

signal is divided, and y_i is the EPR signal magnitude at point i .

The same result may also be derived theoretically in a much simpler way than in reference 41. The differential equation describing an RC type time constant circuit is

$$\frac{dV_o}{dt} = \frac{V_i - V_o}{T} \quad (13)$$

where V_i and V_o are the input and output signals respectively, and T is the time constant.

At times $t' = 0$ and $t' = t_1$, the magnetic field value is outside the EPR spectrum at points of negligible signal; in between these limits, the field is swept through the resonance. Integrating equation 13 gives

$$\frac{1}{T} \int V_i dt' - \frac{1}{T} \int V_o dt' = V_o \quad (14)$$

The constant of integration is zero since all the terms in equation 14 are zero at $t' = 0$. Integrating equation 14 with respect to t from $t = 0$ to $t = t_1$ gives

$$\frac{1}{T} \int_{t=0}^{t_1} \int_{t'=0}^t V_i dt' dt - \frac{1}{T} \int_{t=0}^{t_1} \int_{t'=0}^t V_o dt' dt = \int_0^{t_1} V_o dt = 0. \quad (15)$$

The right side of equation 15 is zero because $\int V_o dt$ is simply a distorted absorption curve which is zero at both of the indicated limits. Thus equation 15 also gives the above-mentioned result.

The operating precision of this electronic double integrator is $\pm 5-10\%$.

SAMPLES

For holding the sample, 3 mm I.D., 4 mm O.D. quartz tubes have been used; they are filled with sample solution, degassed by several freeze-pump-thaw cycles and sealed off under vacuum; used as a standard in the back of the dual cavity has been the Varian strong pitch in KCl sample (a 3 mm I.D., 4 mm O.D. quartz tube) which has been photostable for hundreds of hours. An attempt was made to use sample tubes slightly larger (4 mm I.D., 6 mm O.D.) than the standard sample tube because stronger EPR signals are generally obtained. However, a correction factor for the differences in volume of sample and volume of quartz between the two sizes of tubes was found to vary by $\pm 30\%$ for the several samples run, contrary to our expectation. Due to this variation, which is probably caused by the problem of inhomogeneous light absorption described below, only sample tubes of the standard size are now used.

This simple procedure is not without drawbacks. For one, $[R\cdot]_{SS}$ has been found, in some cases, to decrease significantly during accumulation of an average decay curve by the CAT. This is presumably due to depletion of starting material in the sample tube and consequent reduction in light absorption. If one makes the simplest approximation that $[R\cdot]_{SS}$ decreases linearly with time, then, for the case of second-order decay, an analytic expression for the averaged curve can be calculated as follows.

Defining the second-order decay kinetics as in equation 3, the

solution to the differential equation is

$$[R\cdot] = \frac{[R\cdot]_{SS}}{1 + 2k[R\cdot]_{SS}t} \quad (16)$$

or

$$\frac{[R\cdot]_{SS}}{[R\cdot]} = 1 + 2k[R\cdot]_{SS}t \quad (17)$$

where $[R\cdot] = [R\cdot]_{SS}$ at $t = 0$, which is the start of a decay. The signal which is the input to the CAT is, of course, proportional to $[R\cdot]$. Making the approximation that $[R\cdot]_{SS}$ decreases linearly with time, one can write

$$[R\cdot]_{SS} = [R\cdot]_{SS}^0 (1 - aT) \quad (18)$$

where T is time, and a is a constant. The averaged decay curve accumulated by the CAT memory is then given by

$$[R\cdot] = \frac{1}{T_f} \int_{T=0}^{T_f} \frac{[R\cdot]_{SS}^0 (1 - aT)}{1 + 2kt[R\cdot]_{SS}^0 (1 - aT)} dT \quad (19)$$

where T_f is the total time of accumulation. The value of $[R\cdot]_{SS}$ changes by small increments at a very slow rate compared to the rate of a single radical decay, and therefore equation 19 is an excellent approximation. Integration of equation 19 yields the following expression:

$$[R\cdot] = \frac{2kt[R\cdot]_{SS}^0 a T_f + \ln\left(1 - \frac{2kt[R\cdot]_{SS}^0 a T_f}{1 + 2kt[R\cdot]_{SS}^0}\right)}{(2kt)^2 [R\cdot]_{SS}^0 a T_f} \quad (20)$$

Thus the actual curve stored by the CAT is given by equation 20.

From equation 20, as $t \rightarrow \infty$, $[R\cdot] \rightarrow 0$; also, as $t \rightarrow 0$, $[R\cdot] \rightarrow [R\cdot]_{SS}^0 \left(1 - \frac{a T_f}{2}\right)$. This latter value is the apparent steady-state concentration, designated $[R\cdot]_{SS}'$. From equation 20, we have then

$$\frac{[R\cdot]_{SS}'}{[R\cdot]} = \frac{(2kt[R\cdot]_{SS}^0)^2 a T_f \left(1 - \frac{a T_f}{2}\right)}{2kt[R\cdot]_{SS}^0 a T_f + \ln\left(1 - \frac{2kt[R\cdot]_{SS}^0 a T_f}{1 + 2kt[R\cdot]_{SS}^0}\right)} \quad (21)$$

Expanding the right side of equation 21 about zero in powers of the fractional decrease in $[R\cdot]_{SS}$, i. e., $(a T_f)$, yields

$$\frac{[R\cdot]_{SS}'}{[R\cdot]} = 1 + 2kt[R\cdot]_{SS}^0 - \frac{2kt[R\cdot]_{SS}^0}{2} a T_f + \frac{2kt[R\cdot]_{SS}^0}{12(1 + 2kt[R\cdot]_{SS}^0)} (a T_f)^2 + \dots \quad (22)$$

$$= 1 + 2kt[R\cdot]_{SS}^0 \left[1 - \frac{a T_f}{2} + \frac{(a T_f)^2}{12(1 + 2kt[R\cdot]_{SS}^0)} + \dots \right] \quad (23)$$

Neglect of the square term on the right side of equation 23 is seen to

cause an error of less than 5% for $(aT_f) \leq 0.6$, and therefore to a very good approximation we have

$$\frac{[R\cdot]'_{SS}}{[R\cdot]} = 1 + 2kt[R\cdot]'_{SS} \quad (24)$$

which is of the same form as equation 17. Thus the averaged curve is still very nearly second-order; this is also found experimentally. It is merely necessary to use as the effective $[R\cdot]_{SS}$ the average of the initial and final values.

A second problem with the sample tubes is more serious. The strength of an EPR signal is proportional to the number of free radicals present; in order to calculate the concentration of free radicals, it is obviously necessary to know the volume. In our experiments, the simplest way to do this, and the only way to get good second-order decay kinetics, is to generate free radicals homogeneously throughout the sensitive volume of the sample. Therefore, the optical density, and thus the concentration, of the sample must be low enough to permit approximately uniform light absorption throughout this volume. Of course, it is also necessary to have the sample concentration sufficiently high to complete the experiment before all the starting material is gone. With our setup, these two requirements were mutually exclusive for some chemical systems, and good second-order decay curves were not obtainable.

A third problem arises from variability in the dimensions of ordinary quartz tubing, which was found to cause errors of $\pm 5-10\%$.

The obvious solution to these three problems is to use a slow-flow system (17, 25). The depletion problem is eliminated by continuous renewal of the sample, the inhomogeneous light absorption problem is eliminated by a sufficiently low concentration of sample and the same quartz sample tube is always used. In addition, complications due to absorption of light by products can be minimized.

It is useful to examine the expected dependence of certain quantities on the diameter (d) of the sample tube of such a flow system. This treatment will be for the general kinetics described in the following steady-state equation:

$$\frac{d[R\cdot]}{dt} = \frac{\Phi I}{V} - 2k[R\cdot]_{ss}^2 = 0 \quad (25)$$

The symbol Φ is the quantum yield of free radicals $R\cdot$, I is the light intensity (einsteins/sec) absorbed in the volume V , and k is the bimolecular decay rate constant.

The requirement that light be absorbed (and radicals be generated) approximately homogeneously throughout the sensitive sample volume (V) of cylindrical shape puts an upper limit on the absorbance, and therefore on the product $d \times c$, where c is the sample concentration. Thus, we have the relation

$$c \propto \frac{1}{d} \quad (26)$$

The reasonable assumption will be made that the optics can be adjusted so that I is independent of d. From equation 25, it is seen that

$$[R\cdot]_{ss} \propto \frac{1}{d} \quad (27)$$

The EPR signal strength is very nearly proportional to $[R\cdot]_{ss} \times V$ and therefore to d.

In general, it is desired to follow the radical decay until some very small fraction of the steady-state concentration remains; the time period (τ) for this to occur is easily shown to be proportional to $\frac{1}{[R\cdot]_{ss}}$ and thus to d. Also, a certain signal/noise ratio (s) in the averaged curve is desired, which will require the averaging of N individual decays. Since the signal/noise ratio of one decay is proportional to d as shown above, we have

$$\sqrt{N} \propto \frac{s}{d} \propto \frac{1}{d} \quad (28)$$

In general for real time averaging, the time (T) needed to accumulate one decay is proportional to τ and thus to d. Therefore, the total time for accumulation of N decays is

$$TN \propto \frac{1}{d} \quad (29)$$

The product $c \times$ (volume flow rate) will be independent of d, since it was assumed that I and therefore the depletion rate of starting

material is independent of d . Thus

$$\text{volume flow rate} \propto d \quad (30)$$

The total volume of solution used during the accumulation is then independent of d .

Therefore, it is desirable to use a flow tube of large diameter in order to increase signal strength and decrease the time for doing the experiment, while still expending the same volume of solution.

DISCUSSION

An example of output data is shown in Fig. 4. By locating the lines of zero and maximum (steady-state) signal, the ordinate can be converted into a concentration scale, going from $[R\cdot] = 0$ to $[R\cdot] = [R\cdot]_{SS}$. In this case of second-order decay, the curve yields a value for $k[R\cdot]_{SS}$, where k is the bimolecular rate constant. The value of $[R\cdot]_{SS}$ is measured separately and then k can be calculated.

Measurement of $[R\cdot]_{SS}$ is done as follows: first, the double integral of the sample in the front cavity and the first derivative of the standard pitch sample in the back cavity are simultaneously recorded. The height of the sample double integral is designated $(D.I.)_1$, and the peak-to-peak distance of the first derivative curve is designated $(S.P.)_1$. Then the second standard pitch sample is put into the front cavity, and its double integral is simultaneously recorded along with the first derivative of the standard pitch sample in the back cavity. The height of this double integral is designated $(D.I.)_2$,

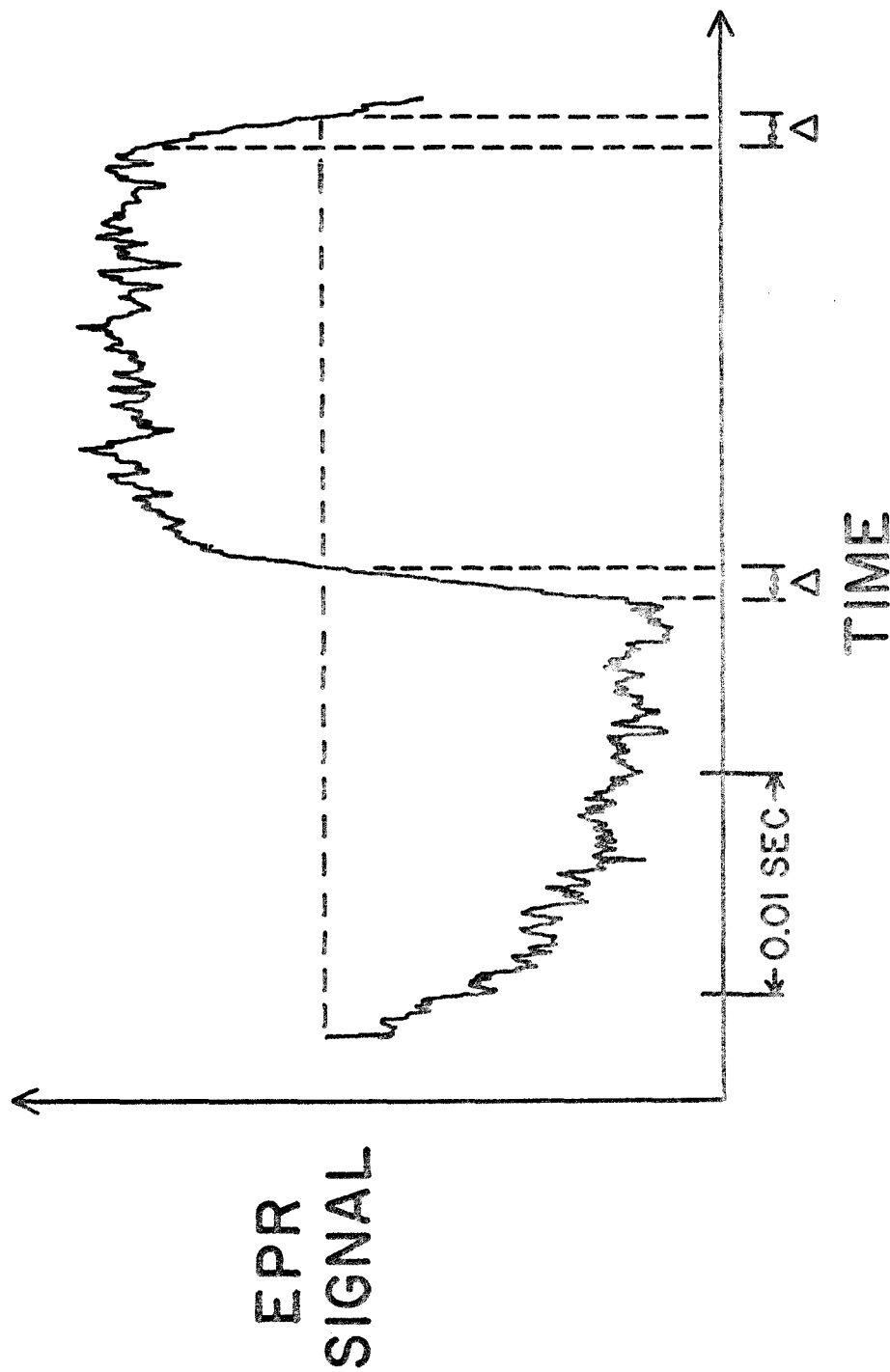


Figure 4. An example of data output from the CAT memory, for the photoreduction of camphorquinone in isopropyl alcohol (42, 37). Shown is the average of 512 transient EPR signals due to the intermediate semidione free radical. The period of the rotating sector is slightly less than the memory width. During the time periods marked Δ , the light intensity is changing and the curve is not useful.

and the peak-to-peak distance of the first derivative curve is designated $(S.P.)_2$. The modulation amplitude for the back cavity should be the same for both scans; also, $(D.I.)_2$ and $(S.P.)_2$ must be corrected for any change in signal levels, magnetic field scan rate or front cavity modulation amplitude. Also, the sample tube must be of the same dimensions as the standard tubes or else an appropriate correction made. Then $[R\cdot]_{SS}$ is given by

$$[R\cdot]_{SS} = \frac{(D.I.)_1 \times (S.P.)_2}{(S.P.)_1 \times (D.I.)_2} \times 7.0 \times 10^{-5} M \quad (31)$$

where $7.0 \times 10^{-5} M$ is the spin concentration of the standard pitch sample, determined by comparison with a known diphenylpicrylhydrazyl (DPPH) solution. It should be noted that the simultaneous measurement of the resonances of the two standard pitch samples is done to compensate for day-to-day changes in the 100 kHz unit of our spectrometer. Theoretically, only one such calibration run need be done.

In the example shown in Fig. 4, $k = 4.2 \times 10^7 M^{-1} \text{ sec}^{-1}$, which is a relatively slow rate of decay. In the case of faster rate constants, of course, the EPR signal is weaker and accumulation of more transients is necessary for good signal/noise ratio. Bimolecular rate constants up to diffusion-controlled can be measured by this method.

It is clearly desirable to have the ratio of Δ , the time of transition from light to dark (or vice versa), to the total sector

period as small as possible, in order to minimize loss of information. This is accomplished by focusing the beam to small size at the sector and making the diameter of the sector as large as is compatible with the rest of the physical dimensions of the system.

REFERENCES

1. P. S. Dixon, A. P. Stefani, and M. Szwarc, J. Am. Chem. Soc., 85, 2551 (1963).
2. W. A. Pryor, "Free Radicals", McGraw-Hill, Inc., New York, N.Y., 1966, p. 313.
3. J. G. Calvert and J. N. Pitts, "Photochemistry", John Wiley and Sons, Inc., New York, N.Y., 1966, section 6-7B-4b, p. 651.
4. See for example, D. J. Carlsson and K. U. Ingold, J. Am. Chem. Soc., 90, 7047 (1968); D. J. Carlsson, J. A. Howard, and K. U. Ingold, ibid., 88, 4726 (1966); ibid., 88, 4725 (1966); R. D. Burkhart, J. Am. Chem. Soc., 90, 273 (1968).
5. See for example, Part II of this thesis; A. Beckett and G. Porter, Trans. Faraday Soc., 59, 2038 (1963).
6. See for example, R. L. McCarthy and A. MacLachlan, Trans. Faraday Soc., 56, 1187 (1960).
7. R. W. Fessenden and R. H. Schuler, J. Chem. Phys., 39, 2147 (1963).
8. R. W. Fessenden, J. Phys. Chem., 68, 1508 (1964).
9. B. Smaller, J. R. Remko, and E. C. Avery, J. Chem. Phys., 48, 5174 (1968).
10. A. J. Parker, D. C. Lainé, and D. J. E. Ingram, J. Sci. Instr., 43, 688 (1966).
11. E. W. Firth and D. J. E. Ingram, J. Sci. Instr., 44, 821 (1967).

12. T. J. Bennett, R. C. Smith, and T. H. Wilmshurst, Chem. Comm., 513 (1967); ibid., Proc. Roy. Soc., A302 305 (1968).
13. T. J. Bennett, R. C. Smith, and T. H. Wilmshurst, J. Sci. Instr., 2, 393 (1969).
14. (a) P. W. Atkins, K. A. McLauchlan, and A. F. Simpson, Chem. Comm., 179 (1968); (b) ibid., "Molecular Spectroscopy", P. Hepple, Ed., The Institute of Petroleum, London, Eng., 1968, pp. 177-184; (c) ibid., Nature, 219, 927 (1968).
15. J. Sohma, T. Komatsu, and Y. Kanda, Japan. J. Appl. Phys., 7, 298 (1968).
16. C. Mazza and K. W. Bowers, Bull. Am. Phys. Soc., 13, 170 (1968).
17. R. Livingston and H. Zeldes, J. Chem. Phys., 44, 1245 (1966).
18. Ibid., 45, 1946 (1966).
19. Ibid., J. Am. Chem. Soc., 88, 4333 (1966).
20. Ibid., J. Chem. Phys., 47, 1465 (1967).
21. Ibid., 47, 4173 (1967).
22. T. A. Claxton, T. E. Gough, and M. C. R. Symons, Trans. Faraday Soc., 62, 279 (1966).
23. T. E. Gough, ibid., 62, 2321 (1966).
24. T. A. Claxton, J. Oakes, and M. C. R. Symons, ibid., 63, 2125 (1967).

25. R. Wilson, J. Chem. Soc. (B), 84 (1968).
26. Ibid., 1581 (1968).
27. R. S. Davidson, et al., J. Chem. Soc. (D), 732 (1969).
28. P. J. Krusic and J. K. Kochi, J. Am. Chem. Soc., 90, 7155 (1968).
29. Ibid., 90, 7157 (1968).
30. J. K. Kochi, P. J. Krusic, and D. R. Eaton, J. Am. Chem. Soc., 91, 1877 (1969).
31. Ibid., 91, 1879 (1969).
32. P. J. Krusic, J. P. Jesson, and J. K. Kochi, J. Am. Chem. Soc., 91, 4566 (1969).
33. E. J. Hamilton, Jr., D. E. Wood, and G. S. Hammond, Rev. Sci. Instr., submitted.
34. S. A. Weiner and G. S. Hammond, J. Am. Chem. Soc., 90, 1659 (1968); ibid., 91, 986 (1969).
35. Ibid., 91, 2182 (1969).
36. Ibid., in press.
37. B. M. Monroe and S. A. Weiner, J. Am. Chem. Soc., 91, 450 (1969); S. A. Weiner, E. J. Hamilton, Jr., and B. M. Monroe, ibid., in press.
38. T. Fujisawa, B. M. Monroe, and G. S. Hammond, J. Am. Chem. Soc., submitted.
39. S. A. Weiner and G. S. Hammond, in preparation.
40. M. L. Randolph, Rev. Sci. Instr., 31, 949 (1960).
41. P. H. Verdier, E. B. Whipple, and V. Schomaker, J. Chem.

Phys., 34, 118 (1961).

42. B. M. Monroe, S. A. Weiner, and G. S. Hammond, J. Am. Chem. Soc., 90, 1913 (1968).

PART II

TERMINATION RATES OF SUBSTITUTED BENZO-
PHENONE KETYL RADICALS IN ALKANES

INTRODUCTION

The photoreduction of benzophenone is one of the most studied of all photoreactions (1). Any one of several types of hydrogen donors may be used, and benzpinacol is usually a major (or the only) product derived from benzophenone. The generally accepted mechanism for this photoreduction, insofar as the production of benzpinacol is concerned, is shown in the following reactions, where RH is a hydrogen donor.



The products of reactions 1 and 2 are, respectively, the lowest excited singlet and triplet states ($\pi^* - n$) of benzophenone.

Recently, Weiner and Hammond (2) have measured the absolute rate constants for the bimolecular decay of ketyl radicals generated by photoreduction of benzophenone and several other ketones, mainly substituted benzophenones. In one series of experiments, benzophenones were photoreduced by the corresponding benzhydrols in benzene solution; in such systems, the only radical present in significant quantities is then the corresponding ketyl radical, which disappears only by bimolecular reaction with itself, thus simplifying the

interpretation of radical decay data (3). In the series of six p-substituted benzophenones examined, termination rate constants were found to vary considerably, from $2.5 \times 10^8 \text{ M}^{-1} \text{ sec}^{-1}$ for 4-bromobenzophenone ketyl radical to $6.4 \times 10^9 \text{ M}^{-1} \text{ sec}^{-1}$ for 4,4'-dimethoxybenzophenone ketyl radical. (Although these values are expected to be only semi-quantitative for reasons discussed elsewhere (4), the existence of a large substituent effect seems definite.) In a second series of experiments, these authors photoreduced several benzophenones in 2-propanol; once again, the bimolecular decay rates of the intermediate ketyl radicals showed a substantial substituent effect. The bimolecular rate constants ranged from $3.4 \times 10^7 \text{ M}^{-1} \text{ sec}^{-1}$ for 4-cyanobenzophenone ketyl radical to $4.8 \times 10^8 \text{ M}^{-1} \text{ sec}^{-1}$ for 3,4-dimethylbenzophenone ketyl radical (the above parenthetical remark also applies here).

As discussed by Weiner and Hammond (2), these large substituent effects are surprising, as were those found in their study (5) of the bimolecular decay rates of cumyl and a series of related radicals. It was expected that such p-substituent effects should be only a minor perturbation on the rates of fast, highly exothermic reactions. Although the observed behavior is not easily explained, the authors present some qualitative ideas. One possible explanation mentioned is that solvent relaxation during radical coupling might be important. When two sp^2 carbon radicals couple, the groups on each central carbon atom move from a trigonal planar configuration to a tetrahedral configuration. This process requires, in general, solvent molecule

reorientation as well, and ease of reorientation might be a critical function of the shape and size of the solvent molecules.

In order to investigate the importance of solvent relaxation, it was decided to measure the bimolecular decay rates of appropriate substituted benzophenone ketyl radicals in a series of alkanes. If variation of alkane solvent caused changes in decay rate that could not be accounted for by the different diffusion rates in the different solvents, then solvent relaxation effects might be demonstrated. Flash photolysis (6) was chosen as the method for the determination of these rates. Although a flash photolysis experiment yields the bimolecular decay rate constant divided by the extinction coefficient of the radical at the monitoring wavelength, rather than the rate constant itself, this was not considered a serious drawback, since the extinction coefficient of a radical should not vary greatly from one alkane solvent to another. The ketones chosen for study and the termination rate constants (2) of the corresponding ketyl radicals in benzene are: benzophenone, $1.8 \times 10^9 \text{ M}^{-1} \text{ sec}^{-1}$; 4,4'-dichlorobenzophenone, $3.3 \times 10^8 \text{ M}^{-1} \text{ sec}^{-1}$; 4,4'-dimethoxybenzophenone, $6.4 \times 10^9 \text{ M}^{-1} \text{ sec}^{-1}$.

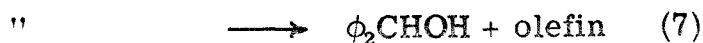
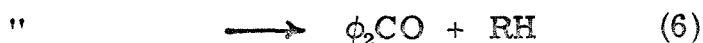
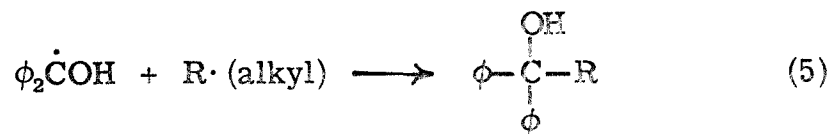
The relevant chemistry of these three compounds and the subject of diffusion control of reaction rates in solution will now be successively reviewed.

Chemical Aspects

Benzophenone has been shown to photoreduce in a number of alkanes with the formation of benzpinacol (7, 8). Although the photo-

reduction in alkanes of neither 4,4'-dichlorobenzophenone nor 4,4'-dimethoxybenzophenone has been reported, these reactions would be expected to occur, since both ketones are known to photoreduce with pinacol formation in other hydrogen-donor solvents (9-11).

In the photoreduction of benzophenone by an alkane solvent, alkyl radicals will be produced in the hydrogen atom abstraction step (reaction 3). Therefore, the possibility arises that the reaction of ketyl radicals with alkyl radicals may be competitive with ketyl-ketyl termination in determining the overall rate of disappearance of ketyl radicals. Three such reactions are plausible:



Very few studies have been carried out which are useful in assessing the importance of these reactions. Walling and Gibian (8) photo-reduced benzophenone in cyclohexane and reported only benzpinacol and bicyclohexyl as products; they specifically stated that no cyclohexene or benzhydrol was detected. Beckett and Porter (12) suggested the occurrence of reaction 6 to explain the fact that the quantum yield for disappearance of benzophenone in n-hexane is less than one. It has been found that coupling is significant between benzophenone ketyl radical and 1-phenyl- or 1,1-diphenyl-substituted alkyl radicals when

benzophenone is photoreduced by the corresponding hydrocarbons (13, 9). On the basis of available studies, therefore, one can only conclude that any or all of reactions 5, 6, and 7 may be important in the photoreduction of benzophenone in alkanes. This statement also applies to the other two ketones in this study.

Using the flash photolysis technique, two groups have determined and assigned the optical absorption spectrum of benzophenone ketyl radical in various solvents (14,12, 15). A maximum is found at 545 nm, essentially independent of solvent. Using kinetic spectrophotometry, bimolecular decay rate constants for this radical were also determined. We define a bimolecular rate constant (k_{obs}) for the reaction



by the following equation:

$$-\frac{1}{2} \frac{d[\text{X}\cdot]}{dt} = k_{\text{obs}} [\text{X}\cdot]^2 \quad (9)$$

In the case at hand, $\text{X}\cdot$ is the benzophenone ketyl radical. Beckett and Porter (12) determined ϵ at 545 nm for this radical in 2-propanol as equal to $5.1 \times 10^3 \text{ M}^{-1} \text{ cm}^{-1}$, using a method involving equating the total amount of benzophenone consumed by several flashes with the total amount of benzophenone ketyl radical observed after the flashes. Using this value of ϵ , they found $k_{\text{obs}} = 3 \times 10^7 \text{ M}^{-1} \text{ sec}^{-1}$ in 2-propanol. Bell and Linschitz (15) determined k_{obs}/ϵ at 545 nm in benzene, and, by assuming that $k_{\text{obs}} = 2 \times 10^9 \text{ M}^{-1} \text{ sec}^{-1}$, calculated a value of

$1.2 \times 10^4 \text{ M}^{-1} \text{ cm}^{-1}$ for ϵ at 545 nm. The rate constant for benzophenone ketyl radical termination measured by Weiner and Hammond (2) is $1.8 \times 10^9 \text{ M}^{-1} \text{ sec}^{-1}$, in very good agreement with the value assumed by Bell and Linschitz.

Diffusional Aspects

The translationally dynamic character of molecules in the liquid state has been realized since the discovery and explanation of Brownian Motion. The equations governing macroscopic translational diffusion in liquids are given by Fick's laws of diffusion, which are based on a continuum model of the liquid. The first law is

$$\vec{J} = - D_{12} \vec{\nabla} c \quad (10)$$

and the second law is

$$\frac{\partial c}{\partial t} = \vec{\nabla} \cdot (D_{12} \vec{\nabla} c) \quad (11)$$

In these equations, c is the concentration of the diffusing substance, D_{12} is the mutual diffusion coefficient of this substance in the given solvent, and \vec{J} is the vector flux of the diffusing substance. In general, D_{12} is a function of concentration; the limiting value of D_{12} as $c \rightarrow 0$ is designated D_{12}^0 . Solutions to equations 10 and 11 have been obtained for a variety of boundary conditions (16). Various methods have been employed for measuring D_{12} (17), including the elegant technique of photochemical space intermittency developed by R. M. Noyes (18), by which direct measurement of the diffusion coefficient of radical inter-

mediates in solution can be accomplished.

Since relatively few measurements of diffusion coefficients have been made, methods for their estimation are important. Reid and Sherwood (19) have recently reviewed critically the many methods for estimation of diffusion coefficients. They recommend use of the empirical relation due to Scheibel (20) for the estimation of mutual diffusion coefficients in nonaqueous solvents in the temperature range 10°C to 30°C . They further state that this method may be expected to predict values of D_{12}^0 with an average absolute error of less than 20%. The Scheibel equation is

$$D_{12}^0 = \frac{KT}{\eta_2 \tilde{V}_1^{\frac{1}{3}}} \quad (12)$$

where

$$K = 8.2 \times 10^{-10} \left(1 + \frac{3\tilde{V}_2}{\tilde{V}_1} \right)^{\frac{2}{3}} \quad (13)$$

The units of D_{12}^0 are $\text{cm}^2 \text{sec}^{-1}$. Subscripts 1 and 2 refer to solute and solvent respectively; η is the viscosity in poise, and \tilde{V} is the molar volume at the normal boiling point as estimated from the atomic volume contributions tabulated by Le Bas (19). For benzene, if $\tilde{V}_1 < 2\tilde{V}_2$, then $K = 18.9 \times 10^{-10}$; for other nonaqueous solvents, if $\tilde{V}_1 < 2.5\tilde{V}_2$, then $K = 17.5 \times 10^{-10}$. The Scheibel method is a modification of that of Wilke and Chang (21).

The most commonly used method of estimating diffusion coefficients is by the Stokes-Einstein equation (22) which, for solute and solvent molecules of comparable size, is

$$D_{12}^0 = \frac{RT}{4\pi N_0 \eta_2 r_1} \quad (14)$$

where r_1 is the radius of the (spherical) solute molecules. If we approximate r_1 by $\frac{1}{2} \left(\frac{\tilde{V}_1}{N_0} \right)^{\frac{1}{3}}$, then equation 14 becomes

$$D_{12}^0 = \frac{RT}{4\pi N_0 \eta_2} 2 \left(\frac{N_0}{\tilde{V}_1} \right)^{\frac{1}{3}} = 1.86 \times 10^{-9} \frac{T}{\eta_2 \tilde{V}^{\frac{1}{3}}} \quad (15)$$

This equation is seen to be nearly identical to the small solute form of the Scheibel equation above.

In a liquid, when two diffusing molecules reach adjacent positions, this event is called an encounter. Because the mean free path is quite short in the liquid phase, a pair of adjacent molecules will generally undergo several collisions with each other before diffusing apart. This phenomenon of multiple collisions of two molecules during an encounter is called the "cage effect", and the two molecules are said to be in a "cage" formed by surrounding molecules. If we consider a bimolecular reaction which involves bond formation and/or bond breaking, it is obviously necessary that two reactable molecules become nearest neighbors before the chemical reaction has any chance to occur. Therefore, in liquid solutions, we may regard such a bimolecular reaction as being composed of two consecutive processes: the (reversible) formation of encounter pairs followed by chemical reaction of such pairs. An important kinetic parameter of such a reaction is the fraction of the total number of encounter pairs formed which react to give products. This brings us to consideration of the

often used term "diffusion-controlled reaction". The most common meaning of this expression as used in the literature will be adopted here: a diffusion-controlled reaction is one in which all encounter pairs of reactants formed go on to give products. Thus, in a diffusion-controlled reaction, the rate of product formation is equal to the rate of encounter of reactants.

The average duration of an encounter between two molecules depends on the magnitude of the diffusion coefficient of these molecules in the solvent used; a higher diffusion coefficient results in a lower encounter duration. Assuming that the solvent doesn't affect the rate constant for encounter pairs reacting to give products, it is then clear that a given bimolecular reaction may be diffusion-controlled in one solvent and not diffusion-controlled in a second solvent in which the diffusion coefficient is larger and diffusion of reactants out of the cage competes significantly with chemical reaction. By the same token, if the diffusion coefficient can be lowered sufficiently by choice of solvent, any bimolecular reaction will become diffusion-controlled.

The effect of diffusion rate on the observed rate constant of a bimolecular chemical reaction in solution has been reviewed (23-25). Noyes (25) has derived the following equation for the rate constant (k) of a bimolecular reaction between identical species, where k is defined as in equation 9.

$$k = \frac{\frac{4\pi N_0 \rho D_{12}^0}{1000}}{1 + \frac{4\pi N_0 \rho D_{12}^0}{1000 k_c}} \quad (16)$$

The symbol ρ is the encounter diameter of (spherical) reactants (center to center distance at closest approach), and k_c is the rate constant which would be observed if diffusion were sufficiently fast that the distribution of remaining reactant molecules at any time was that given by equilibrium statistical mechanics. If the reaction is between two different reactants, then D_{12}^0 in equation 16 is replaced by the sum of the mutual diffusion coefficients of the two reactants. The approximations and assumptions in the derivation have been thoroughly discussed (25); the poorest approximation may be to assume that the motions of nearby reactant molecules are uncorrelated (26).

As explained above, $k = k_c$ at the high D_{12}^0 limit. If a reaction occurs on every encounter at this limit, then k_c may be set equal to the gas phase collision rate constant from the kinetic theory of gases (25).

$$k_c = k_c^0 = 2 \left(\frac{\pi RT}{M} \right)^{\frac{1}{2}} \rho^2 \frac{N_0}{1000} \quad (17)$$

Here M is the molecular weight of reactant. Of course, a reaction that occurs on every encounter at the high D_{12}^0 limit will also be 100% efficient at lower D_{12}^0 values where encounters are of longer duration. Thus, if k_c^0 is substituted for k_c in equation 16, we have the following

expression for k_D , the diffusion-controlled rate constant.

$$k_D = \frac{\frac{4\pi N_0 \rho D_{12}^0}{1000}}{1 + \frac{4\pi N_0 \rho D_{12}^0}{1000 k_c^0}} \quad (18)$$

This equation may be compared with the earlier expression for the rate constant of a diffusion-controlled reaction due to Smoluchowski (27):

$$k_D = \frac{4\pi N_0 \rho D_{12}^0}{1000} \quad (19)$$

This equation, derived using an incorrect boundary condition (28), is seen by comparison with equation 18, to be valid only when $1000 k_c^0 \gg 4\pi N_0 \rho D_{12}^0$, a condition which is not always fulfilled (23-25).

EXPERIMENTAL

Ketones

Benzophenone was commercial material recrystallized from ligroin by L. J. Sharp, IV.

4, 4' -Dichlorobenzophenone was obtained from Aldrich Chemicals Company; it was sublimed twice at $\sim .05$ mm Hg pressure and $135-140^{\circ}$ C bath temperature. Melting point $145.1-146.2^{\circ}$ C.

4, 4' -Dimethoxybenzophenone was also obtained from Aldrich and purified in the same way as the previous compound. Melting point $142.1-144.7^{\circ}$ C.

Alkanes

Cyclopentane, 2, 2, 4-trimethylpentane (except as below), methylcyclohexane, cyclohexane, and n-hexadecane were Spectro-quality Solvents from Matheson, Coleman, and Bell, used without further purification.

2-Methylbutane (MC & B, Spectroquality), n-pentane (Phillips Petroleum Company, Pure Grade), except as below, and n-hexane (Phillips, Pure Grade) were further purified by stirring over concentrated H_2SO_4 for several days. The acid was changed several times until it was no longer darkened appreciably by reaction. The alkane was then decanted, washed twice with aqueous Na_2CO_3 solution, washed once with water, dried over anhydrous $MgSO_4$, and distilled from P_2O_5 at atmospheric pressure. The n-hexane was purified by H. L. Hyndman.

In the last stages of this work, the new procedure of Murray and Keller (29) for alkane purification was used. Basically, it involves passing an alkane, previously dried over P_2O_5 , through a

silver nitrate on alumina column. n-Pentane (Phillips, Pure Grade) and 2, 2, 4-trimethylpentane (MC & B, Spectroquality) were purified in this way and used for the flash photolysis of 4, 4' -dichlorobenzophenone and 4, 4' -dimethoxybenzophenone, respectively.

Sample Preparation

The dissolving of 4, 4' -dichlorobenzophenone and 4, 4' -dimethoxybenzophenone in the alkane solvents usually was hastened by warming the solution. Sample cells were cylinders made of Pyrex; their length was ~21 cm and diameter ~1 cm. Sample solutions in sidearms of such cells were degassed by four freeze-pump-thaw cycles and sealed off under a vacuum of 10^{-4} mm Hg or better.

Flash Photolysis - Kinetic Spectrophotometry

The apparatus and procedures have been described in detail previously (30,6), so only a brief description is given here. Two xenon flash lamps were situated parallel to the sample cell and provided the exciting light. A second lamp, continuously operated, was located at one end of the sample cell on the axis and provided a "monitor" beam for the observation of the decay of transient absorptions resulting from the exciting flash. The light of the monitor beam which was transmitted by the sample along its axis was passed through a monochromator set for a certain wavelength. The intensity of the light at this wavelength was measured by a photomultiplier tube whose output as a function of time was displayed on an oscilloscope. Oscilloscope traces were photographed with a Polaroid camera; the negatives were projected onto a large screen and data points read off.

Flash Photolysis - Flash Spectroscopy

In this type of experiment (also called "double" flash photolysis), two xenon flash lamps were situated parallel to the sample cell and provided the exciting light, just as for kinetic spectrophotometry. Another, smaller, flash lamp was located at one end of the sample cell on the axis and provided a "monitor" flash (at a specified time after the exciting flash) for the observation of the absorption spectra of transients resulting from the exciting flash. The light from the monitor flash which was transmitted by the sample along its axis was passed through a Bausch and Lomb Two Meter Prism Spectrograph onto an Eastman Kodak Type 103a-F Spectrographic Plate. Wavelength calibration of the plate was achieved from the mercury lines of a BLE Spectroline Model SCT-1 low pressure mercury pencil light which was shined through the entrance slit of the spectrograph onto appropriate places on the plate. Plates were developed and fixed, and then plate blackening was quantitatively determined by a Jarrell-Ash High Precision Recording Microphotometer, Model 23-500.

RESULTS

Ultraviolet Absorption Spectra of Ketones

Ultraviolet absorption spectra above about 300 nm are shown in Figure 1 for the three ketones studied; they were recorded at about 25° C on a Cary 14 Recording Spectrophotometer from 2.56×10^{-3} M solutions in cyclohexane. The $\pi^* \leftarrow n$ singlet state

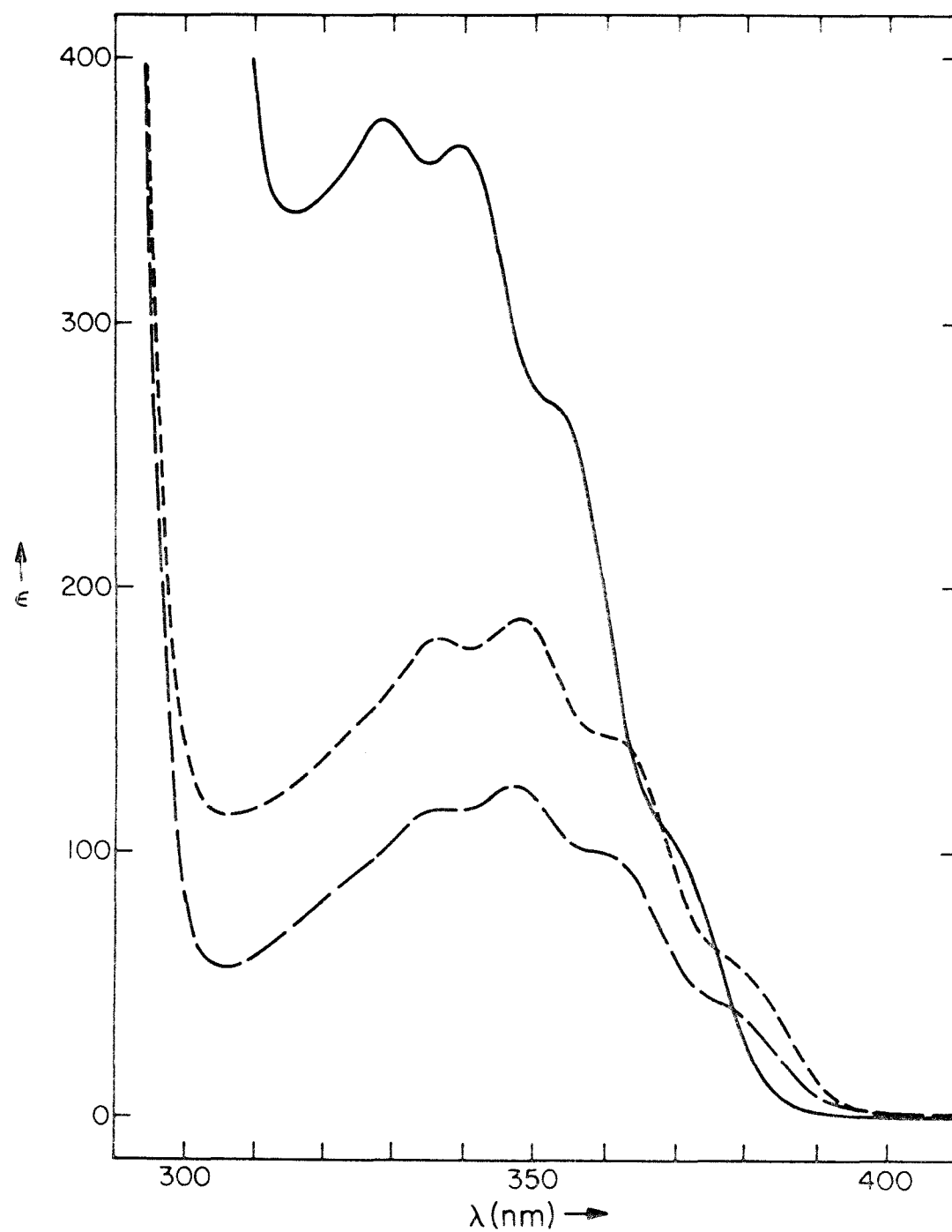


Figure 1. Ultraviolet absorption spectra of benzophenone (— — —), 4,4'-dichlorobenzophenone (---), and 4,4'-dimethoxybenzophenone (— · —) in cyclohexane at about 25° C.

is seen to be the lowest excited singlet state in all three cases.

In the flash photolysis apparatus, the monitoring beam or flash passes through the sample along the axis, and therefore only transients formed near the axis are detected. Thus, the concentration of light absorbing species in the sample must be sufficiently low to allow enough exciting light to reach the sample axis so transients may be detected. This consideration puts an upper limit on the absorbance of sample solutions.

The Pyrex sample cells are essentially opaque to wavelengths less than 280 nm. From the spectra in Figure 1, it may be estimated that, for light passed by Pyrex, equiabsorbance solutions of benzophenone, 4,4'-dichlorobenzophenone, and 4,4'-dimethoxybenzophenone will have concentrations in the ratios 3:2:1, respectively.

Flash Photolysis - Spectra

Each of the following solutions was double flashed: 1.0×10^{-2} M benzophenone in n-hexane and in cyclohexane, 6.7×10^{-2} M 4,4'-dichlorobenzophenone in n-hexane and in cyclohexane, 1.0×10^{-3} M 4,4'-dimethoxybenzophenone in n-hexane, and a saturated ($\sim 1.6 \times 10^{-3}$ M) solution of 4,4'-dimethoxybenzophenone in cyclohexane. The spectrum of the monitor flash alone was also recorded in each case for use as a reference. The transmittance of each plate (relative to the unexposed portion of the plate) was recorded as a function of wavelength by the microphotometer. Wavelength calibration was carried out using the 435.8 nm, 546.1 nm, and 577.0 nm mercury lines and the following equation for prism spectrographs due to Hartmann (31):

$$\lambda_d = \lambda_0 + \frac{c}{d_0 - d} \quad (20)$$

In this equation, λ_d is the unknown wavelength at a point a distance d measured from an arbitrary point in the spectrum; λ_0 , c , and d_0 are constants which are evaluated from the locations of the three known wavelengths.

From an inspection of the microphotometer records, the following conclusions could be drawn: the monitor lamp's light output was the same for each flash; there was no apparent difference in the shape of any of the transient spectra due to solvent (n-hexane and cyclohexane), and a 17 μ sec rather than a 40 μ sec delay time between the exciting and monitor flashes resulted only in slightly more transient absorption. It is easily shown (6) that, if the monitor lamp's light output is the same for each flash, and if plate exposure is in the linear region of the characteristic curve (see below), then

$$\epsilon(\lambda) \propto A_{\text{plate}}^{\text{reference}}(\lambda) - A_{\text{plate}}^{\text{double}}(\lambda) \quad (21)$$

where $\epsilon(\lambda)$ is the extinction coefficient of the transient, $A_{\text{plate}}^{\text{reference}}(\lambda)$ is the absorbance of the plate from the reference (monitor) flash, and $A_{\text{plate}}^{\text{double}}(\lambda)$ is the absorbance of the plate from the double flash. The characteristic curve of a photographic plate is a plot of plate absorbance against the logarithm of the exposure time to some source of light; this curve is generally linear only over a limited range of plate absorbance.

The present work did not result in plate absorbances entirely in this linear range, and, therefore, complete spectra of intermediates were not obtained. In order to locate an absorption maximum, which was the purpose of these double flash experiments, it is sufficient that the characteristic curve be essentially linear over the range limited by double flash plate absorbance at the maximum and by reference flash plate absorbance at the same wavelength. This condition was very well fulfilled for the 4, 4'-dimethoxybenzophenone data, and a maximum found at 557.0 nm for the transient. In the case of the benzophenone data, the condition was less well met, but a maximum was nevertheless found at about 545 nm as previously reported for benzophenone ketyl radical (14,12,15). In the case of 4, 4'-dichlorobenzophenone data, the condition was not nearly fulfilled, and the wavelength (588.1 nm) at which the later kinetic experiments were performed is probably not a maximum. The extinction coefficient at λ_{\max} of a spectrum is expected to be more nearly constant in a series of similar solvents than the extinction coefficient at another wavelength.

On the bases of 1) the known photochemistry of these ketones as discussed in the Introduction, 2) the agreement of the observed maximum of the transient absorption in the flash photolysis of benzophenone with the maximum of the absorption spectrum of benzophenone ketyl radical as reported in the literature, and 3) the observed second-order decay of the three transients (see following section), the three observed transient absorptions are assigned to the corresponding ketyl radicals. The relative strengths of the observed absorptions were 4, 4'-dichlorobenzophenone ketyl radical > benzophenone ketyl radical > 4, 4'-dimethoxybenzophenone ketyl radical.

Flash Photolysis - Kinetics

Solutions of each of the three ketones in each of eight alkane solvents were flash photolyzed at $23 \pm 1^\circ \text{C}$, and the decay of intermediate ketyl radicals was followed by kinetic spectrophotometry at wavelengths where neither reactants nor products absorbed.

Table 1

Solution Concentrations and Monitoring Wavelengths		
benzophenone	$1.0 \times 10^{-2} \text{ M}$	546.1 nm
4, 4' -dichlorobenzophenone	$6.7 \times 10^{-3} \text{ M}$	588.1 nm
4, 4' -dimethoxybenzophenone	$1.0 \times 10^{-3} \text{ M}$	557.0 nm

The solubility of 4, 4' -dimethoxybenzophenone in the alkane solvents limited the maximum concentration to below the limit imposed by the equiabsorbance consideration previously discussed (see p. 48). An example of kinetic data is shown in Figure 2, and, as explained in the caption, points giving transmittance as a function of time may be obtained, and the origin of the time scale is arbitrary. As can be judged from Figure 2, an undetermined amount of radical has already reacted before it is possible to take points from the decay curve.

The radical decays were analyzed in terms of second-order kinetics. Second-order decay of the intermediate ketyl radicals ($X\cdot$) has been defined by equation 9. The solution to the differential equation 9 is

Figure 2. An example of flash photolysis kinetic data, from the flash photolysis of 4, 4' -dimethoxybenzophenone in n-hexane at 23° C, monitored at 557.0 nm. Trace A is obtained with the monitor beam blocked. At the beginning, trace A shows the photomultiplier output level when there is no incident light; then the exciting flash occurs, causing the trace to fall so fast as to not be seen; the second part of trace A that is visible shows the decay of the exciting flash and consequent return to the zero incident light level. Trace B is obtained with the monitor beam unblocked. At the beginning, trace B indicates the photomultiplier output level when the 557 nm light of the monitor beam is totally transmitted by the sample; then the exciting flash occurs, causing the trace to drop off the display; the second part of trace B that is visible reveals the existence and decay of a transient which absorbs at 557 nm. The levels of transmittance (T) equals zero and equals one are determined as shown, and thus a plot of transmittance as a function of time for the transient's decay is obtained.

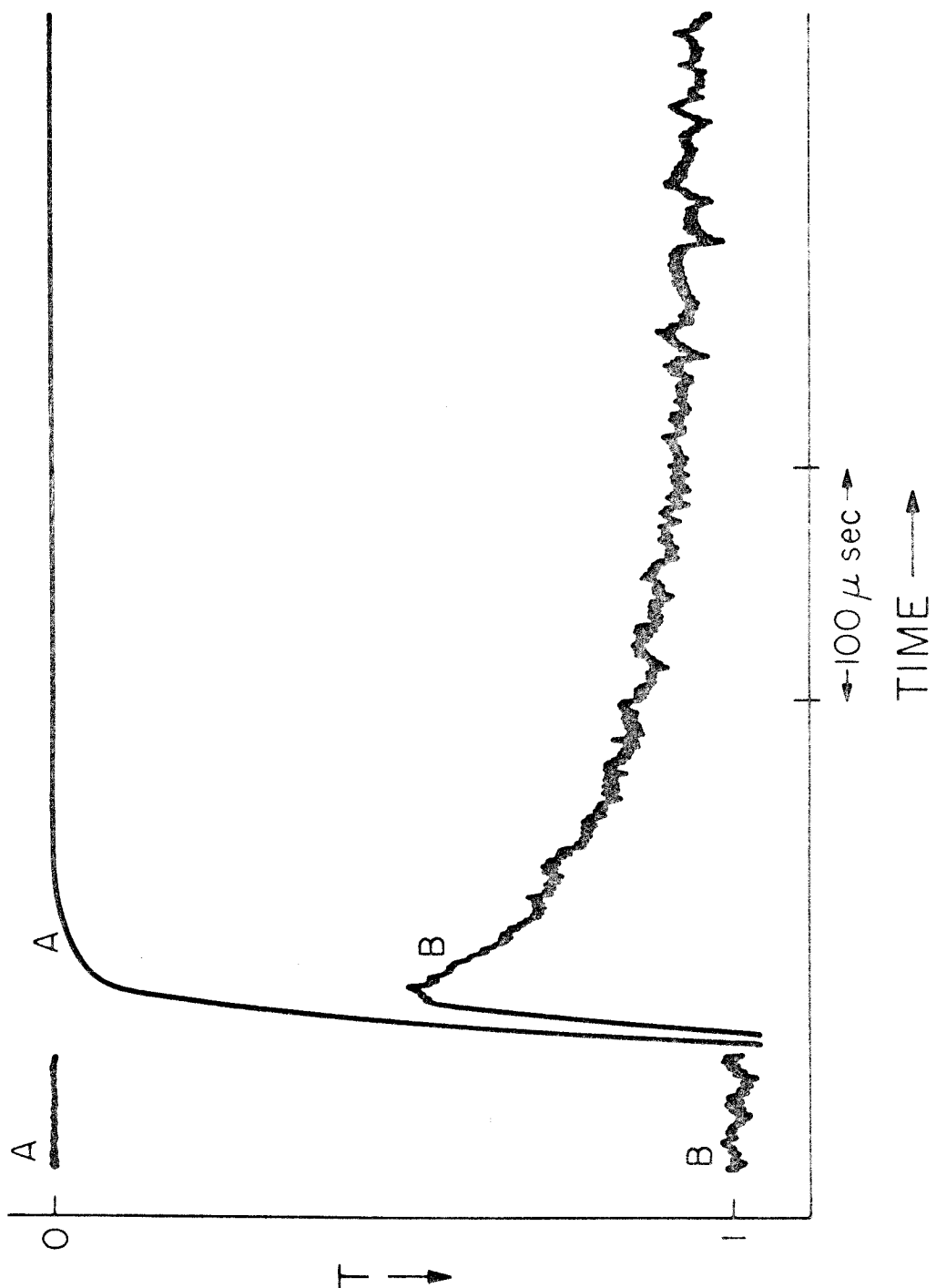


Figure 2. See previous page for caption.

$$\frac{1}{[X \cdot]} = \frac{1}{[X \cdot]_0} + 2 k_{\text{obs}} t \quad (22)$$

where $[X \cdot] = [X \cdot]_0$ at $t = 0$. The transmittance of $X \cdot$ is given by

$$-\log_{10} T = -\log T = \epsilon \ell [X \cdot] \quad (23)$$

where ℓ is the path length, and ϵ is the decadic extinction coefficient of $X \cdot$ at the monitoring wavelength. Solving equation 23 for $[X \cdot]$ and substituting into equation 22, we have

$$\frac{1}{\log T} = \frac{1}{\log T_0} - \frac{2 k_{\text{obs}}}{\epsilon \ell} t \quad (24)$$

where $T = T_0$ at $t = 0$. Thus, knowing ℓ , the slope of a straight line plot of $1/\log T$ versus t permits the determination of k_{obs}/ϵ .

The best value of the slope was determined by the method of least squares, making the excellent approximation that the only source of error is in the values of T . As is well known (32) if the expectation of absolute error is not the same for all points, then each point must be weighted in proportion to the inverse of the square of its standard deviation (σ_i). In the present case, the sum to be minimized may be written

$$S = \sum_{i=1}^n \frac{1}{\sigma_i^2} (Y_i - y_i)^2 \quad (25)$$

where Y_i is the measured value of $1/\log T$ at t_i , and y_i is the calculated value of $1/\log T$ at t_i . The y_i values are calculated from

values of the slope and intercept of the line which are varied to minimize the sum S . Errors in T arise from photomultiplier noise, as shown in Figure 2, and the expectation value of the absolute error (ΔT) is constant for all values of T . We may approximate the resulting error in $1/\log T$ by

$$\Delta \left(\frac{1}{\log T} \right) = \frac{\partial \left(\frac{1}{\log T} \right)}{\partial T} \Delta T \quad (26)$$

$$= - \frac{.4343}{T(\log T)^2} \Delta T \quad (27)$$

Since ΔT is a constant, we may write

$$\frac{1}{\sigma_1^2} \propto T^2(\log T)^4 \quad (28)$$

and substitute into equation 25.

The above computations were done by computer using a program written in CITRAN. Values of k_{obs}/ϵ obtained are shown in Table 2. Fits of the decay data to the second-order kinetics were quite good. The average percent standard errors of k_{obs}/ϵ were 1.0% for benzophenone ketyl radical, 2.0% for 4,4'-dichlorobenzophenone ketyl radical, and 3.3% for 4,4'-dimethoxybenzophenone ketyl radical, and systematic curvature of the $1/\log T$ versus t plots was never observed. The less good fits of the decays of the last two radicals can be ascribed to greater photomultiplier noise than in the case of benzophenone ketyl radical, when a strong mercury line was used as monitor wavelength.

Table 2

Experimental Values of k_{obs}/ϵ for the
Bimolecular Decay of Ketyl Radicals

Solvent Num- bers	$\frac{k_{\text{obs}}}{\epsilon} \times 10^{-6} \text{ (cm sec}^{-1}\text{)}$		
	$(\text{C}_6\text{H}_5)_2 \dot{\text{C}}\text{OH}$	$(\text{Cl-C}_6\text{H}_4)_2 \dot{\text{C}}\text{OH}$	$(\text{CH}_3\text{O-C}_6\text{H}_4)_2 \dot{\text{C}}\text{OH}$
1 2-methylbutane	.67	.34	1.4
2 <u>n</u> -pentane	.62	.36	1.3
3 <u>n</u> -hexane	.57	.29	1.2
4 cyclopentane	.38	.15	.82
5 2, 2, 4-trimethyl- pentane	.55	.25	.83
6 methylcyclohexane	.32	.11	.65
7 cyclohexane	.32	.12	.70
			.55
			(.62 = average)
8 <u>n</u> -hexadecane	.18	.071	.32
			.30
			(.31 = average)

In some cases, points were taken from the decay curve before the exciting flash had completely decayed (see Figure 2). It is easily shown (6) that, if all exciting flashes are of the same intensity, then data from the radical decay curve (trace B) may be corrected by adding on the amount by which the flash decay (trace A) is below the

T = 0 line at the same time. This procedure generally gave points lying on a straight line with the others.

It was found that, for benzophenone ketyl and 4, 4'-dimethoxybenzophenone ketyl radicals, decay data were independent of previous flashing of the sample. However, in the case of 4, 4'-dichlorobenzophenone ketyl radical, a rather precipitous decrease in amount of transient formed and increase in rate of bimolecular decay of that transient occurred in flashes after the first; therefore, the data for this radical shown in Table 2 are all from first flashes.

An approximate constancy was observed in the minimum transmittance values of the decay curves of each ketyl radical in the eight solvents used.

DISCUSSION

Noyes Equation

As described in the Introduction, the equation derived by Noyes (25) that gives the effect of diffusion on the observed rate constant (k) of a bimolecular reaction is

$$k = \frac{\frac{4\pi N_0 \rho D_{12}^0}{1000}}{1 + \frac{4\pi N_0 \rho D_{12}^0}{1000 k_c}} \quad (29)$$

while the relation giving the diffusion-controlled rate constant (k_D) for the same circumstances is

$$k_D = \frac{\frac{4\pi N_0 \rho D_{12}^0}{1000}}{1 + \frac{4\pi N_0 \rho D_{12}^0}{1000 k_c^0}} \quad (30)$$

The symbols k_c and k_c^0 were previously defined. Figures 3 and 4 give plots, according to the above equations, of k and of k_D , respectively, as functions of D_{12}^0 all in appropriate reduced units. The fraction (α) of total encounters which lead to reaction is given by

$$\alpha = \frac{k}{k_D} \quad (31)$$

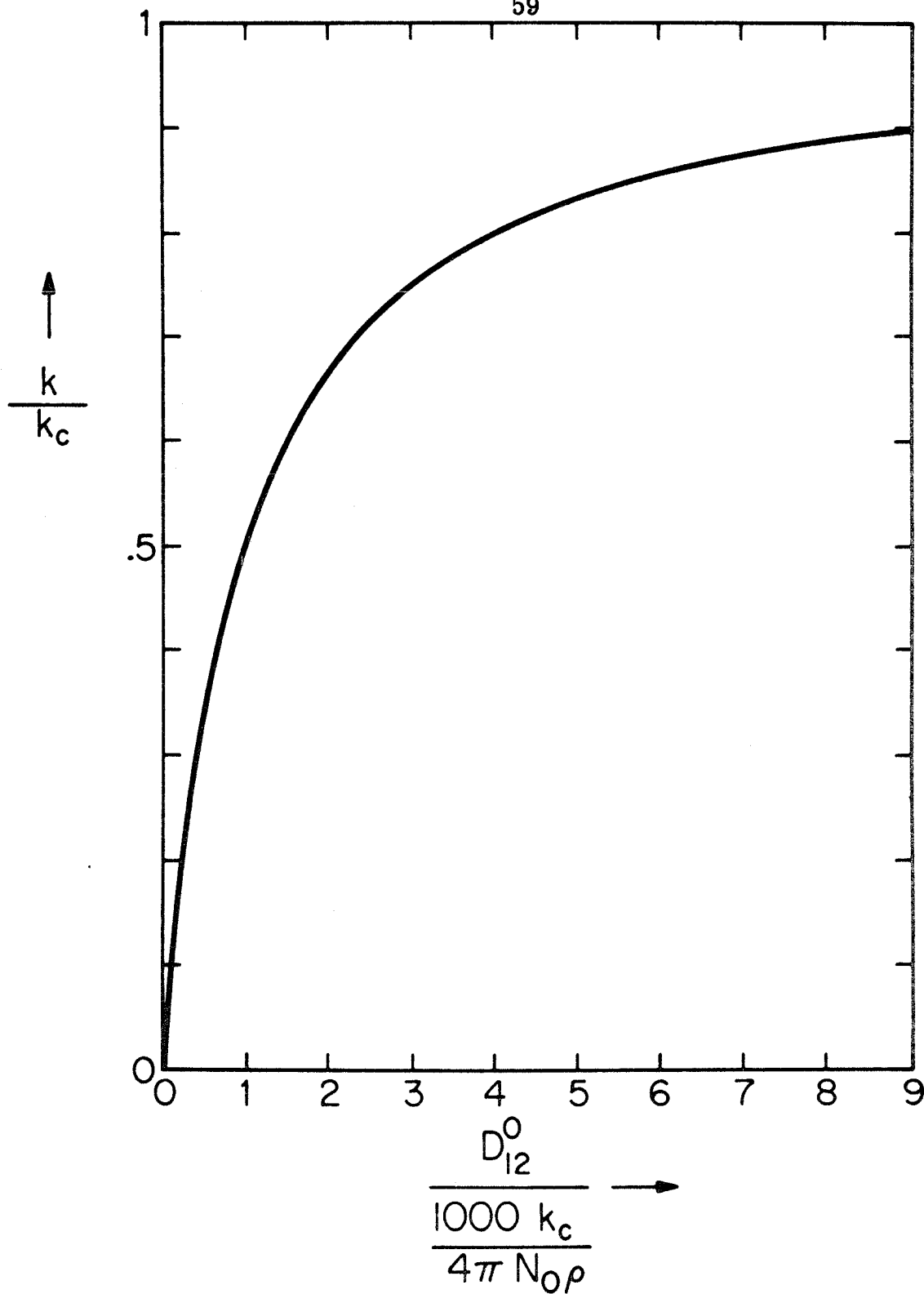


Figure 3. A plot of k as a function of D_{12}^0 , both appropriately reduced, according to equation 29.

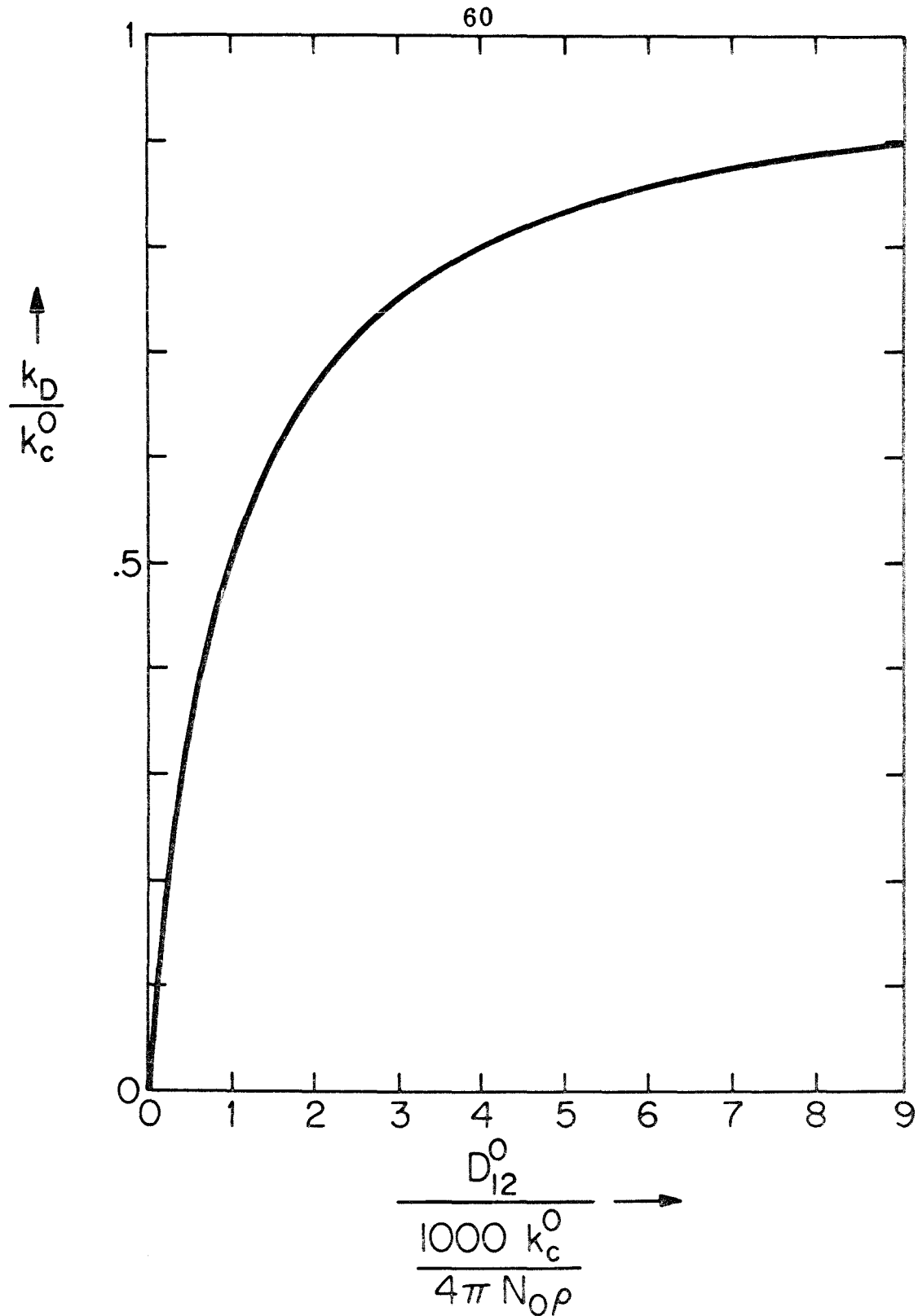


Figure 4. A plot of k_D as a function of D_{12}^0 , both appropriately reduced, according to equation 30.

From equations 29, 30, and 31, we have

$$\alpha = \frac{1 + \frac{4\pi N_0 \rho D_{12}^0}{1000 k_c^0}}{1 + \frac{4\pi N_0 \rho D_{12}^0}{1000 k_c}} \quad (32)$$

Also, the often cited quantity $(\frac{1}{\alpha} - 1)$ may be written as

$$\frac{1}{\alpha} - 1 = \frac{\frac{k_c^0}{k_c} - 1}{\frac{1000 k_c^0}{4\pi N_0 \rho D_{12}^0} + 1} \quad (33)$$

Figures 5 and 6 show plots of α and $(\frac{1}{\alpha} - 1)$ as functions of D_{12}^0 , all in appropriate reduced units.

Interpretation of Data

The estimation of encounter diameters and mutual diffusion coefficients for the self-termination of ketyl radicals will be undertaken first. Table 3 lists the viscosities at the temperature of the kinetic experiments, the Le Bas molar volumes, and the estimated effective diameters of the eight solvents used. The relation which is used for the effective diameter, $\rho = \left(\frac{\tilde{V}}{N_0}\right)^{\frac{1}{3}}$, has often been used in the literature; it is equivalent to assuming cubic packing of spherical molecules. For neopentane, a molecule close to spherical, this relation was found to give a molecular diameter about equal to that

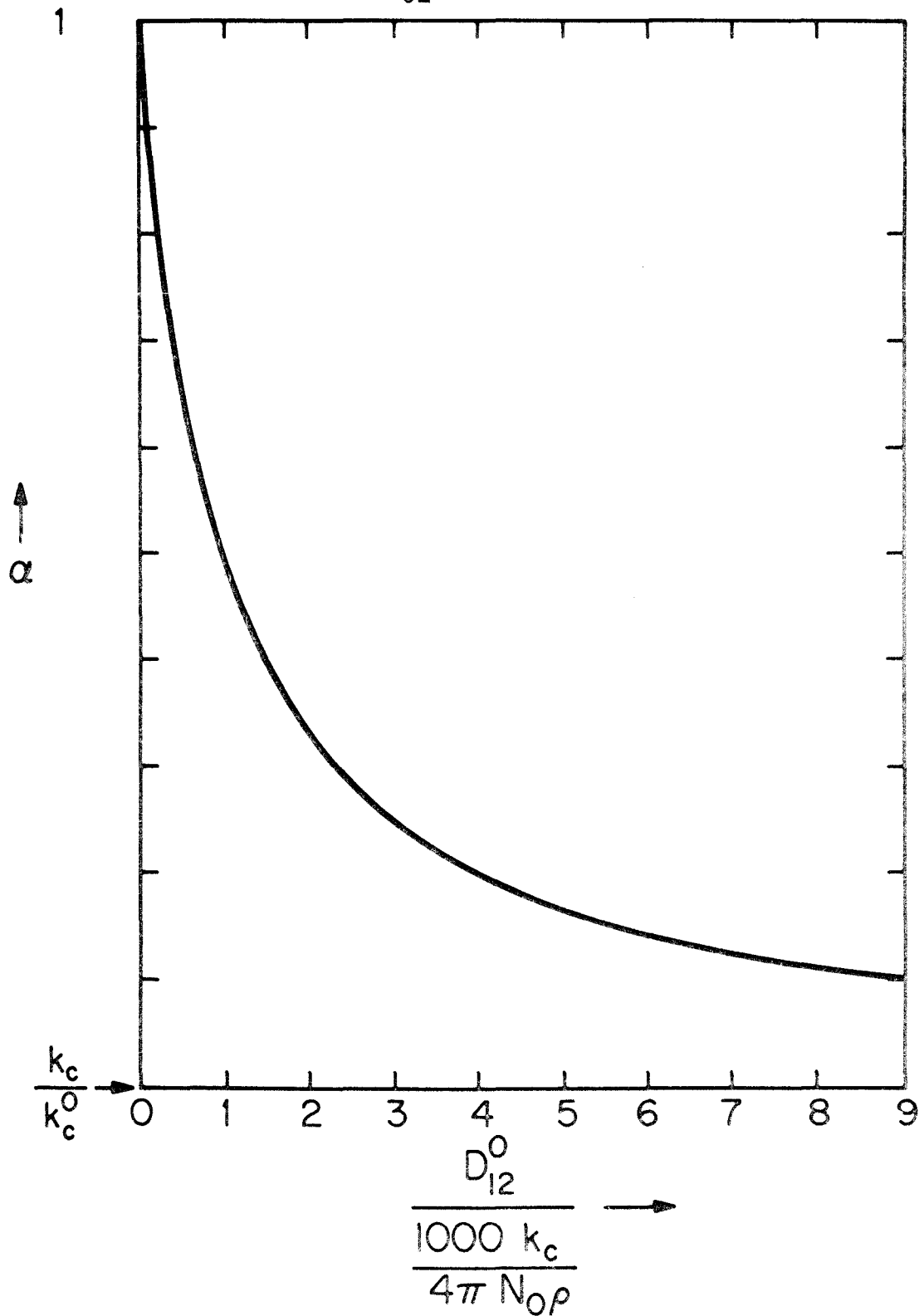


Figure 5. A plot of α as a function of D_{12}^0 , both appropriately reduced, according to equation 32.

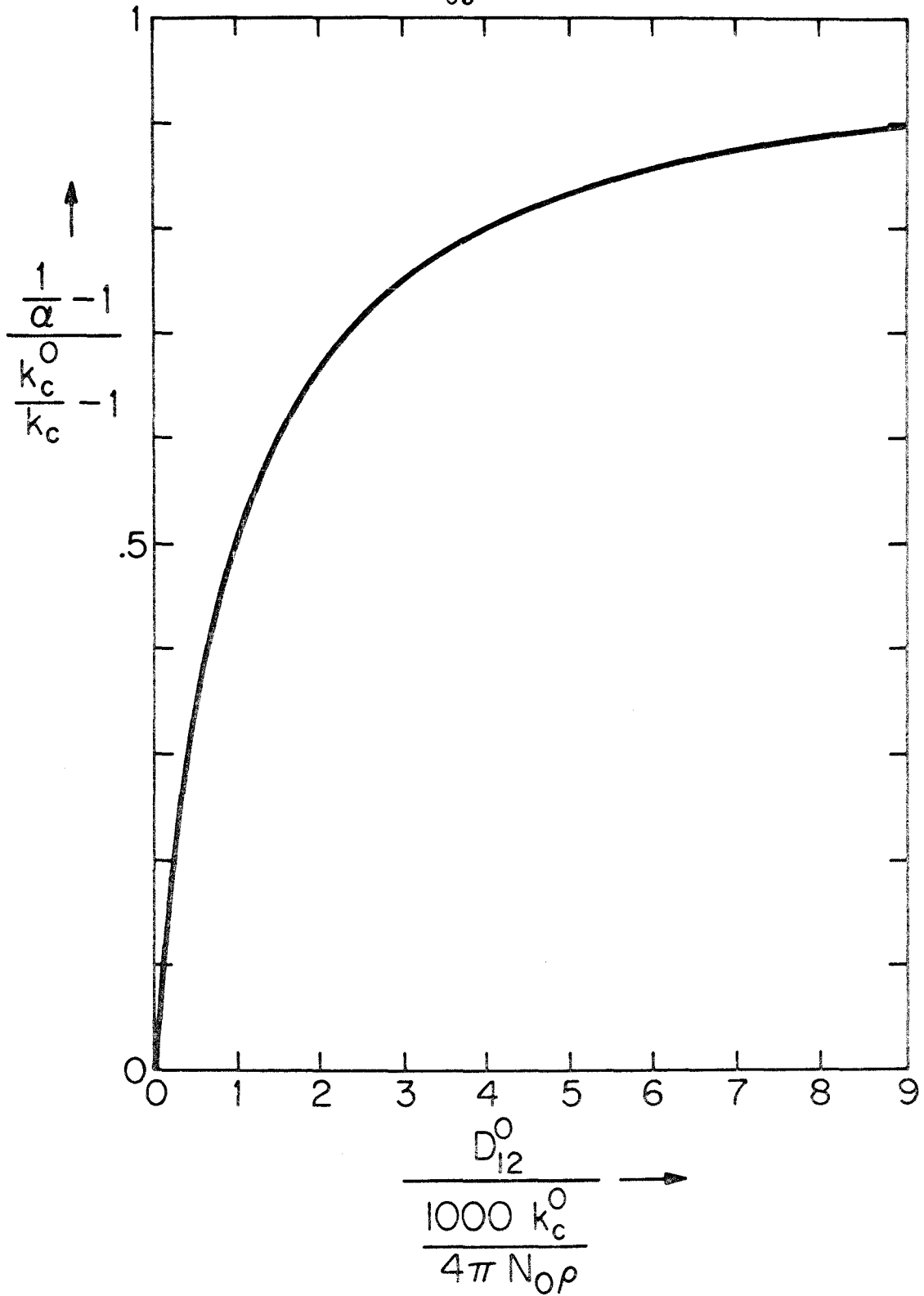


Figure 6. A plot of $(\frac{1}{\alpha} - 1)$ as a function of D_{12}^0 , both appropriately reduced, according to equation 33.

Table 3

Viscosities*, Le Bas Molar Volumes†, and
Estimated Molecular "Diameters"‡ of Solvents

	η (centipoise) at 23° C	\tilde{V} (cm ³ /mole)	ρ (Å)
2-methylbutane	.219	118.4	5.81
<u>n</u> -pentane	.229	118.4	5.81
<u>n</u> -hexane	.304	140.6	6.16
cyclopentane	.425	111.0	5.69
2, 2, 4-trimethylpentane	.482	185.0	6.75
methylcyclohexane	.704	155.4	6.37
cyclohexane	.930	133.2	6.05
<u>n</u> -hexadecane	3.244	362.6	8.44

*Interpolated according to the equation $\ln \eta = \frac{A}{T} + B$ (A and B are constants) (33) from data at 20° C and 25° C from reference 34, except for 2, 2, 4-trimethylpentane, where data at 20° C and 35° C from reference 35 were used.

† From table in reference 19.

$$\ddagger \rho = \left(\frac{\tilde{V}}{N_0} \right)^{\frac{1}{3}} .$$

measured for a CPK space filling model of this molecule; a relation based on the assumption of cubic closest packing gave a less accurate result. Therefore, the former relation is used here. Values of \tilde{V} and ρ for the ketyl radicals are shown in Table 4. Diffusion coefficients, D_{12}^0 , for the ketyl radicals in all solvents except n-hexadecane were calculated using the Scheibel equation, equation 12, described in the Introduction. Since it was found that $\tilde{V}_1 < 2.5 \tilde{V}_2$ for all the ketyl radical-solvent pairs, the following form of the Scheibel equation was used:

$$D_{12}^0 = 1.75 \times 10^{-9} \frac{T}{\eta_2 \tilde{V}_1^{\frac{1}{3}}} \quad (34)$$

In the case of n-hexadecane, a very non-spherical molecule, the work of Gorrell and Dubois (36) suggested a different method of estimation. They measured the diffusion coefficients of several molecules, of similar size to the ketyl radicals of this study, in n-hexadecane and also calculated values for the same coefficients by several literature methods. Best agreement with the experimental data was obtained using the equation

$$D_{12}^0 = \frac{RT}{4\pi N_0 \eta_2 r_1 f} \quad (35)$$

where

$$f = 0.16 + 0.4 \frac{r_1}{r_2} \quad (36)$$

Table 4

Calculated Ketyl Radical Parameters

	M.W.	$\tilde{V}(\text{cm}^3/\text{mole})^\dagger$	$\rho(\text{\AA})^\ddagger$	k_c^0 ($\text{M}^{-1} \text{sec}^{-1}$)
$(\text{C}_6\text{H}_5)_2\dot{\text{C}}\text{OH}$	183	210.5	7.04	1.22×10^{11}
$(\text{Cl-C}_6\text{H}_4)_2\dot{\text{C}}\text{OH}$	252	252.3	7.48	1.18×10^{11}
$(\text{CH}_3\text{O-C}_6\text{H}_4)_2\dot{\text{C}}\text{OH}$	243	274.7	7.70	1.28×10^{11}

[†]From table in reference 19.

$$\ddagger \rho = \left(\frac{\tilde{V}}{N_0} \right)^{\frac{1}{3}}$$

where r_1 and r_2 are the estimated (by the same method as above for ρ) radii of solute and solvent molecules respectively. The quantity f is the coefficient of microfriction introduced by Gierer and Wirtz (37). Values of D_{12}^0 , calculated as has been described, are listed in Tables 5, 6, and 7. Using these values together with the k_c^0 values from Table 4, values of k_D for ketyl radical self-termination may be calculated using equation 18; they are also listed in Tables 5, 6, and 7.

The kinetic results for ketyl radical ($\text{X}\cdot$) decay indicated that, during the part of the decay observed, the disappearance of ketyl radicals is described very well by the rate law

Table 5

Calculated Diffusion-Dependent Quantities for
the Self-Termination of Benzophenone Ketyl Radicals

	$D_{12}^0 \times 10^5$ ($\text{cm}^2 \text{sec}^{-1}$)	$\frac{1000}{4\pi N_0 \rho D_{12}^0} \times 10^{10}$ (M sec)	$k_D \times 10^{-10}$ ($\text{M}^{-1} \text{sec}^{-1}$)
2-methylbutane	3.98	.473	1.80
<u>n</u> -pentane	3.80	.494	1.74
<u>n</u> -hexane	2.86	.656	1.35
cyclopentane	2.05	.918	1.00
2, 2, 4-trimethylpentane	1.81	1.04	.891
methylcyclohexane	1.24	1.52	.624
cyclohexane	.936	2.01	.479
<u>n</u> -hexadecane	.576	3.26	.299

$$-\frac{1}{2} \frac{d[\text{X}\cdot]}{dt} = k_{\text{obs}}[\text{X}\cdot]^2 \quad (37)$$

As related in the Introduction, the reaction of ketyl radicals both with other ketyl radicals and with alkyl radicals ($\text{R}\cdot$) derived from the solvent is possible in the systems studied. The rate law would then be expected to be

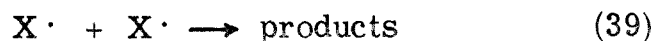
Table 6

Calculated Diffusion-Dependent Quantities for the Self-Termination of 4, 4' -Dichlorobenzophenone Ketyl Radicals

	$D_{12}^0 \times 10^5$ (cm ² sec ⁻¹)	$\frac{1000}{4\pi N_0 \rho D_{12}^0} \times 10^{10}$ (M sec)	$k_D \times 10^{-10}$ (M ⁻¹ sec ⁻¹)
2-methylbutane	3.74	.473	1.79
<u>n</u> -pentane	3.58	.494	1.73
<u>n</u> -hexane	2.70	.656	1.35
cyclopentane	1.93	.918	.998
2, 2, 4-trimethylpentane	1.70	1.04	.889
methylcyclohexane	1.16	1.52	.623
cyclohexane	.882	2.01	.478
<u>n</u> -hexadecane	.521	3.40	.287

$$-\frac{1}{2} \frac{d[X\cdot]}{dt} = k_1 [X\cdot]^2 + \frac{k_2}{2} [X\cdot][R\cdot] \quad (38)$$

where k_1 is the rate constant for the reaction



and k_2 is the rate constant for the reaction

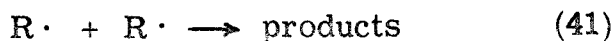


Table 7

Calculated Diffusion-Dependent Quantities for the Self-Termination of 4, 4' -Dimethoxybenzophenone Ketyl Radicals

	$D_{12}^0 \times 10^5$ ($\text{cm}^2 \text{sec}^{-1}$)	$\frac{1000}{4\pi N_0 \rho D_{12}^0} \times 10^{10}$ (M sec)	$k_D \times 10^{-10}$ ($\text{M}^{-1} \text{sec}^{-1}$)
2-methylbutane	3.64	.473	1.82
<u>n</u> -pentane	3.48	.494	1.75
<u>n</u> -hexane	2.62	.656	1.36
cyclopentane	1.88	.918	1.01
2, 2, 4-trimethylpentane	1.65	1.04	.894
methylcyclohexane	1.13	1.52	.626
cyclohexane	.857	2.01	.480
<u>n</u> -hexadecane	.496	3.47	.282

Equation 38 will have the same form as equation 37 only if $[R\cdot] = [X\cdot]$ during the part of the decay observed. Since $R\cdot$ and $X\cdot$ are formed in equal amounts by the abstraction reaction, this condition requires that k_3 , the rate constant for the reaction



be equal to k_1 , assuming the only radical destroying processes are reactions 39-41. That such an equality should hold for all the

ketyl-alkyl radical pairs of this investigation seems unlikely. In addition, several literature data make this even less reasonable. Burkhart (38) has recently measured k_3 for cyclohexyl radicals in cyclohexane at 25° C as equal to $0.6 \times 10^9 \text{ M}^{-1} \text{ sec}^{-1}$ and notes that previous measurements of this value are all higher and range up to $2 \times 10^9 \text{ M}^{-1} \text{ sec}^{-1}$. If k_1 were equal to k_3 in this case, then the termination rate constant for 4, 4'-dimethoxybenzophenone ketyl radical in cyclohexane would be much less than the value measured (2) in benzene of $6.4 \times 10^9 \text{ M}^{-1} \text{ sec}^{-1}$. This would be opposite to the ordering previously observed for the several radicals studied in these two solvents (38, 2). Also, the three-fold variation in termination rate constants observed (38, 2) for the n-propyl, t-butyl, and cyclohexyl radicals in cyclohexane is contrary to the assumption of equal alkyl radical reactivity that is implicit in $k_1 = k_3$. Therefore, it is reasonable to assume that the observed ketyl radical disappearance is due only to the reaction of two ketyl radicals--that is, $k_{\text{obs}} = k_1$.

The ketyl radical decay data will now be interpreted using the Noyes equation. Rearranging this equation for k_{obs} and multiplying by ϵ yields the expression

$$\frac{\epsilon}{k_{\text{obs}}} = \epsilon \cdot \frac{1000}{4\pi N_0 \rho D_{12}^0} + \frac{\epsilon}{k_c} \quad (42)$$

As mentioned previously, ϵ is assumed to be independent of alkane solvent; in a study similar to this one, Beckett et al. (39) found such an assumption for $\phi\dot{\text{C}}\text{HOH}$ radical in a series of hydroxylic solvents to be consistent with their data. Figures 7, 8, and 9 show plots for

the three ketyl radicals of ϵ/k_{obs} values from Table 2 against $1000/(4\pi N_0 \rho D_{12}^0)$ values from Tables 5, 6, and 7. (See Table 2, page 56, for solvent numbers) The fact that the points for each ketyl radical can be reasonably well correlated by a straight line indicates no non-systematic variation of ϵ with solvent. Also the straight line correlations indicate that rate constant variations in the different alkane solvents can be accounted for by diffusion rate variations, and, therefore, no solvent relaxation effect is apparent.

Least square fits of straight lines to each of the three sets of points were carried out. The assumption that deviations from a straight line are due only to errors in ϵ/k_{obs} , and that the expectation of absolute error in k_{obs}/ϵ is proportional to k_{obs}/ϵ for all the points, leads to the slopes and intercepts in the first column of Table 8. The assumption that deviations from a straight line are due only to errors in $1000/(4\pi N_0 \rho D_{12}^0)$ arising from errors in D_{12}^0 , and that the expectation of absolute error in D_{12}^0 is proportional to D_{12}^0 , leads to the values in second column of Table 8. For both these fits, points were appropriately weighted using the method outlined on page 54. Judging from the errors to be expected in the estimations of D_{12}^0 (see page 39), and from the reproducibility of k_{obs}/ϵ data (see page 56), the ordinate and abscissa values have roughly the same expectation of error. Therefore, averages of the least square parameters from the two above fits (third column, Table 8) are considered the best values and were used to determine the solid straight lines of Figures 7, 8, and 9. The scatter in the points did not seem to warrant a more accurate least square analysis than the above. Deviations of points from these

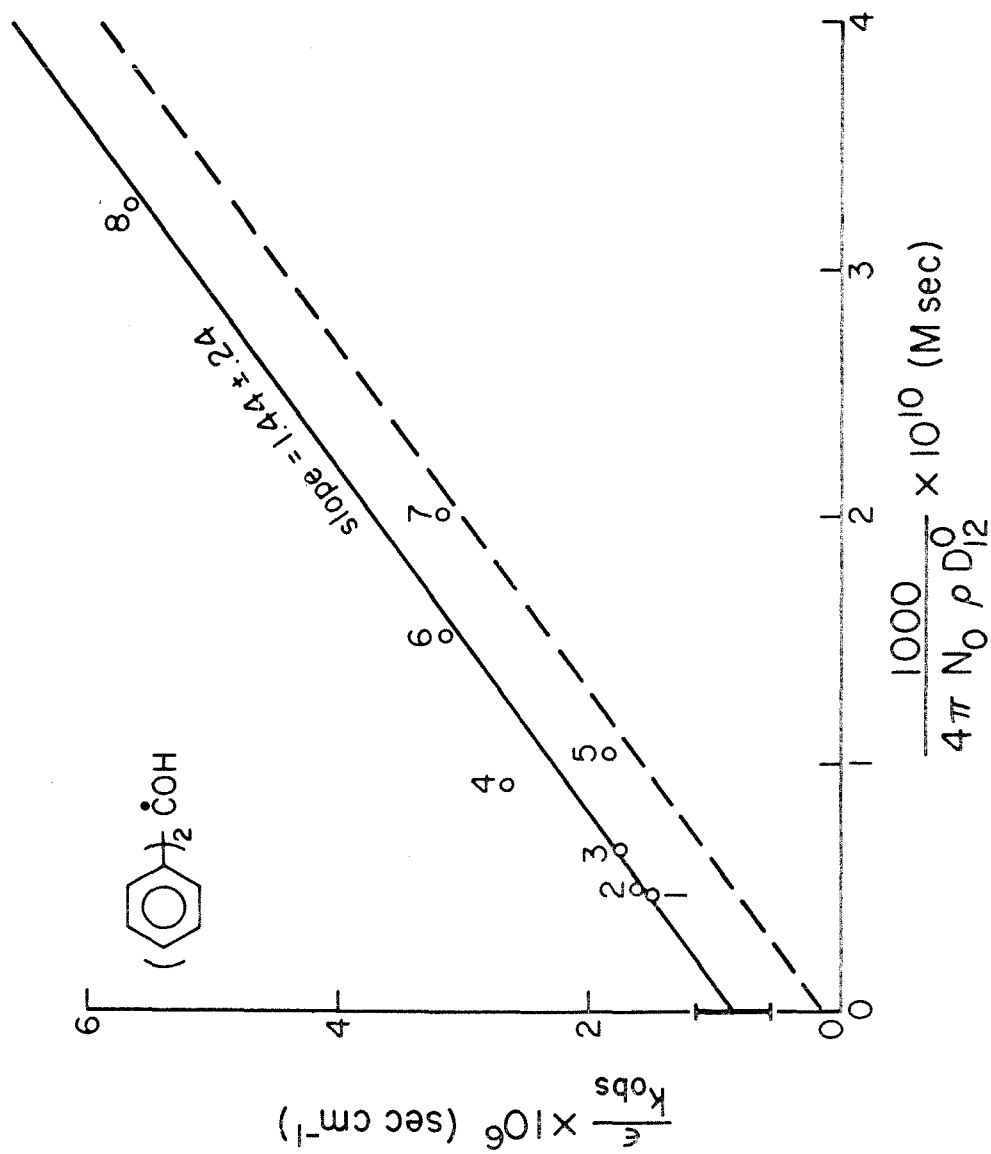


Figure 7. A plot of decay data for benzophenone ketyl radical in several alkanes according to the Noyes equation.

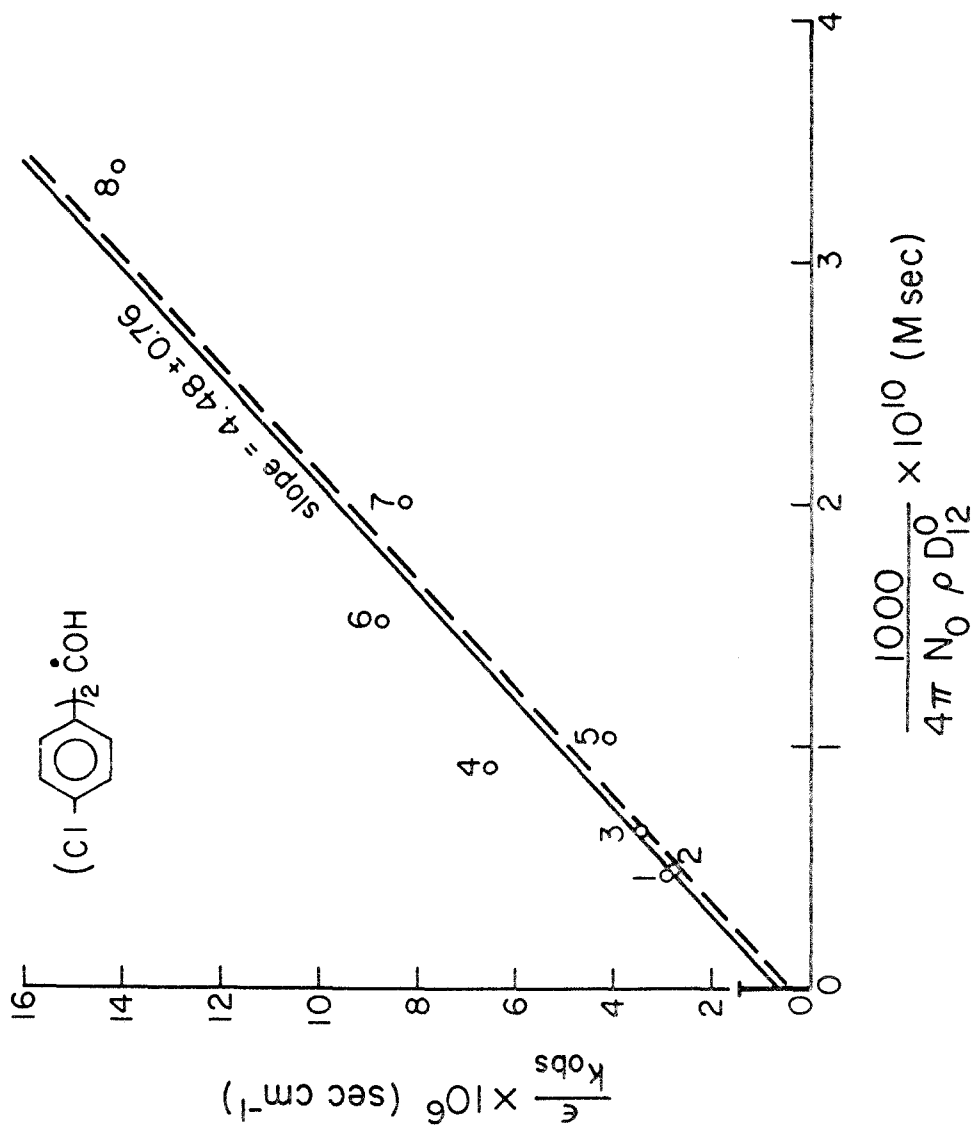


Figure 8. A plot of decay data for 4,4'-dichlorobenzophenone ketyl radical in several alkanes according to the Noyes equation.

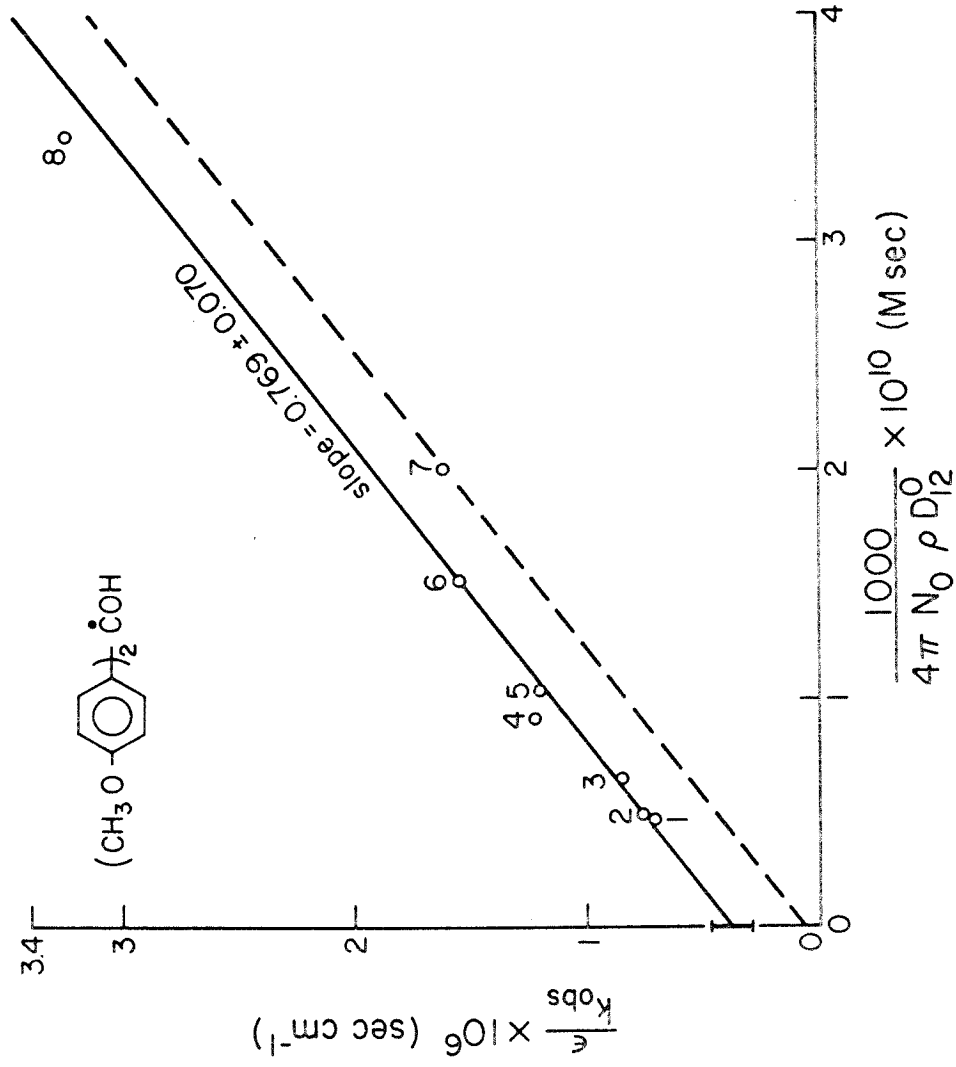
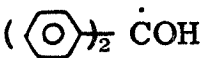
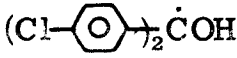



Figure 9. A plot of decay data for 4,4'-dimethoxybenzophenone ketyl radical in several alkanes according to the Noyes equation.

Table 8

Least Square Parameters and Standard
Errors for the Fit of Points to the Equation

$$\frac{\epsilon}{k_{\text{obs}}} \times 10^6 = \text{slope} \times \frac{1000}{4\pi N_0 \rho D_{12}^0} \times 10^{10} + \text{intercept}$$

		Errors in ϵ/k_{obs} only	Errors in $\frac{1000}{4\pi N_0 \rho D_{12}^0}$ only	average
	slope	1.28 ± .21	1.59 ± .28	1.44 ± .24
	intercept	.90 ± .30	.74 ± .30	.82 ± .30
	slope	3.88 ± .61	5.08 ± .90	4.48 ± .76
	intercept	.96 ± .77	.31 ± .87	.63 ± .82
	slope	.733 ± .068	.806 ± .072	.769 ± .070
	intercept	.398 ± .098	.353 ± .081	.376 ± .089

fitted lines are not greater than those expected from the uncertainties in ϵ/k_{obs} and/or $1000/(4\pi N_0 \rho D_{12}^0)$. The error bars on the ordinate axes of these figures show the standard errors of the intercepts.

According to equation 42, the slopes of the fitted straight lines in Figures 7, 8, and 9 give values of ϵ directly; these values are shown in Table 9 along with values of k_c obtained from the intercepts and slopes. The ϵ value of 1.4×10^4 for benzophenone ketyl radical in alkanes agrees well with 1.2×10^4 found in benzene (15), but not with the 5.1×10^3 found in 2-propanol (12). However, the data of Weiner and Hammond (2), which support the above ϵ value in benzene, indicate that the ϵ in 2-propanol is too low; their termination rate constant of $1.1 \times 10^8 \text{ M}^{-1} \text{ sec}^{-1}$ combined with the well known k_{obs}/ϵ value of 5.8×10^3

Table 9

Values of ϵ and k_c and Their Standard Errors

	$\epsilon \times 10^{-3} \text{ (M}^{-1} \text{ cm}^{-1}\text{)}$	$k_c \times 10^{-10} \text{ (M}^{-1} \text{ sec}^{-1}\text{)}$
$(\text{C}_6\text{H}_5)_2 \dot{\text{C}}\text{OH}$	$14.4 \pm 2.4 \text{ at } 546.1 \text{ nm}$	$1.76 \pm .71$
$(\text{CH}_2\text{C}_6\text{H}_4)_2 \dot{\text{C}}\text{OH}$	$44.8 \pm 7.6 \text{ at } 588.1 \text{ nm}$	$7. \pm 9.$
$(\text{CH}_3\text{O-C}_6\text{H}_4)_2 \dot{\text{C}}\text{OH}$	$7.69 \pm .70 \text{ at } 577.0 \text{ nm}$	$2.05 \pm .52$

cm sec⁻¹ (12) yields $\epsilon = 1.9 \times 10^4$, which better agrees with the other two values. Table 10 shows values of k_{obs} obtained by multiplying the experimental values of k_{obs}/ϵ from Table 2 by the ϵ values of Table 9. The dashed lines in Figure 7, 8, and 9 have the same slopes as the corresponding fitted solid lines and have intercepts of ϵ/k_c^0 , values of k_c^0 being taken from Table 4. These dashed lines thus show the calculated diffusion-controlled rates.

The rate constants in Table 10 are seen to be quite similar for the three ketyl radicals in the same alkane solvent, compared to the differences observed in benzene (2). The rate constants for 4,4'-dichlorobenzophenone ketyl radical are seen to be substantially higher in all alkanes than those for the other two radicals. However, the possible significance of these higher rate constants is muddled by the two anomalies associated with the kinetic data for this particular ketyl radical: the monitoring wavelength was probably not a maximum in the absorption spectrum, and decay rates depended on previous

Table 10

Values of k_{obs} for the Bimolecular
Decay of Ketyl Radicals

	$k_{\text{obs}} \times 10^{-10} \text{ (M}^{-1} \text{ sec}^{-1}\text{)}$		
	$(\text{C}_6\text{H}_5)_2 \dot{\text{C}}\text{OH}$	$(\text{Cl-C}_6\text{H}_4)_2 \dot{\text{C}}\text{OH}$	$(\text{CH}_3\text{O-C}_6\text{H}_4)_2 \dot{\text{C}}\text{OH}$
2-methylbutane	.96	1.5	1.1
<u>n</u> -pentane	.89	1.6	1.0
<u>n</u> -hexane	.82	1.3	.92
cyclopentane	.55	.67	.63
2, 2, 4-trimethylpentane	.79	1.1	.64
methylcyclohexane	.46	.49	.50
cyclohexane	.46	.54	.48
<u>n</u> -hexadecane	.26	.32	.24

flashing of the samples. Therefore, it is concluded that there is no measurable substituent effect of p, p' -dimethoxy- and either a relatively small or no substituent effect of p, p' -dichloro- on the self-termination rate constant of benzophenone ketyl radicals in alkanes. Therefore, the large substituent effects on ketyl radical self-termination measured by Weiner and Hammond (2) are substituent-dependent solvent effects.

Based on the fitted lines of Figures 7 and 9 and the k_D values of Tables 5 and 7, values of α , the efficiency of encounters in leading to reaction, for benzophenone ketyl and 4, 4'-dimethoxybenzophenone ketyl radicals are seen to vary from about 0.5 in isopentane to almost 0.9 in n-hexadecane. The k_c values from Table 9 for these two radicals are each about 0.15 times the respective k_c^0 values from Table 4. A comparison of these k_c values with the gas phase rate constants (presently unknown) of the same reactions would be useful in determining if there is any alkane solvent effect. Since diffusion control of a reaction requires that reaction occur even in encounters in which non-reactive parts of reactant molecules become adjacent, it seems likely that orientation factors are responsible for the inefficiency observed for these reactions in alkanes. Because of the large error in k_c (Table 9) and the anomalies mentioned previously, the kinetic data for 4, 4'-dichlorobenzophenone ketyl radical were not included in the above discussion.

Using the estimation methods for ρ and D_{12}^0 that were used earlier, one can compute values of $1000/(4\pi N_0 \rho D_{12}^0)$ for the three ketyl radicals in benzene. From the fitted straight lines of Figures 7, 8, and 9, it is then possible to obtain the rate constants expected for the three ketyl radicals in benzene, if benzene behaved like an alkane solvent in these terminations. Such rate constants are given in Table 11 together with the actually measured values (2). The rate constants for 4, 4'-dimethoxybenzophenone ketyl radical are probably the same within experimental error, while the measured values for the other two radicals are well below the calculated ones. The

Table 11

Rate Constants for Ketyl Radical Termination in Benzene
 $\times 10^{-9} (\text{M}^{-1} \text{sec}^{-1})$

	Calculated for ϕH as an alkane	Measured (in reference 2)
$(\text{C}_6\text{H}_5)_2\dot{\text{C}}\text{OH}$	4.9	1.8
$(\text{CH}_2\text{C}_6\text{H}_4)_2\dot{\text{C}}\text{OH}$	5.9	.33
$(\text{CH}_3\text{O-C}_6\text{H}_4)_2\dot{\text{C}}\text{OH}$	4.8	6.4

ordering of the ratios of measured to calculated rate constants for the three radicals supports the idea (2) that charge transfer complexing between ketyl radicals (acceptors) and benzene (donor) is responsible for observed substituent effects in that solvent.

In an experiment not detailed in this Thesis, it was found that the decay rates in 2-propanol of benzophenone ketyl and benzophenone- d_{10} ketyl radicals were identical (and in good agreement with the reported value (12) for the former). This result suggests that the intramolecular transfer of excess vibrational energy in ketyl radical coupling in 2-propanol is not rate-limiting.

All of the above data interpretation has been in terms of the Noyes equation and depends on the accuracy of that equation. It may

be noted that the data support the validity of the Noyes equation only in that the predicted straight line plots of non-zero intercept were obtained.

Conclusions

The main conclusions of the second part of this Thesis will be briefly noted. The self-termination rate constants divided by ϵ of benzophenone ketyl and 4, 4' -dichloro- and 4, 4' -dimethoxy-benzophenone ketyl radicals were measured in a series of eight alkanes. Rate variations were satisfactorily accounted for by diffusion coefficient variations according to the equation derived by R. M. Noyes. No solvent relaxation effect was apparent. Values of ϵ were extracted from the data using the Noyes equation. The ϵ (at 546.1 nm) value thus obtained for benzophenone ketyl radical in alkanes was in reasonable agreement with literature values for this radical in other solvents.

The absolute rate constants obtained showed no substituent effect on benzophenone ketyl radical termination in alkanes. Thus, the previously observed effects in other solvents are substituent-dependent solvent effects. Evidence was cited for the observed effects in benzene being due to charge-transfer complexing between radical and solvent. The absolute rate constants for the termination of the three ketyl radicals in alkanes were all at least about 0.5 times, but clearly less than, the corresponding diffusion-controlled rate constants.

REFERENCES

1. Extended discussion and pertinent references may be found in recent books: D. C. Neckers, "Mechanistic Organic Photochemistry", Reinhold Publishing Corporation, New York, 1967, p. 163; J. G. Calvert and J. N. Pitts, Jr., "Photochemistry", John Wiley and Sons, Inc., New York, 1966, p. 532; R. O. Kan, "Organic Photochemistry", McGraw-Hill Book Company, New York, 1966, p. 222; N. J. Turro, "Molecular Photochemistry", W. A. Benjamin, Inc., New York, 1965, p. 139.
2. S. A. Weiner and G. S. Hammond, J. Am. Chem. Soc., in press.
3. W. M. Moore, G. S. Hammond, and R. P. Foss, ibid., 83, 2789 (1961).
4. See Part I of this Thesis, p. 20.
5. S. A. Weiner and G. S. Hammond, J. Am. Chem. Soc., 91, 986 (1969).
6. See for example, G. Porter, "Flash Photolysis", in S. L. Friess, E. S. Lewis, and A. Weissberger, editors, Investigation of Rates and Mechanisms of Reactions, 2nd edition, (Vol. VIII of Technique of Organic Chemistry), Part II, Interscience, New York, N. Y., 1963, pp.1055-1106.
7. E. Paterno and G. Chieffi, Gazz. chim. ital., 39b, 415 (1909).
8. C. Walling and M. J. Gibian, J. Am. Chem. Soc., 87, 3361 (1965).

9. G. S. Hammond, W. P. Baker, and W. M. Moore, J. Am. Chem. Soc., 83, 2795 (1961).
10. J. N. Pitts, Jr., H. W. Johnson, Jr., and T. Kuwana, J. Phys. Chem., 66, 2456 (1962).
11. H. W. Johnson, Jr., J. N. Pitts, Jr., and M. Burleigh, Chem & Ind. (London), 1493 (1964).
12. A. Beckett and G. Porter, Trans. Faraday Soc., 59, 2038 (1963).
13. A. Schonberg and A. Mustafa, Chem. Revs., 40, 181 (1947).
14. G. Porter and F. Wilkinson, Trans. Faraday Soc., 57, 1686 (1961).
15. J. A. Bell and H. Linschitz, J. Am. Chem. Soc., 85, 528 (1963).
16. J. Crank, "The Mathematics of Diffusion", Oxford University Press, New York, 1956.
17. See for example, A. L. Geddes and R. B. Pontius, "Determination of Diffusivity", in A. Weissberger, editor, Physical Methods of Organic Chemistry, 3rd edition, (Vol. I of Technique of Organic Chemistry), Part II, Interscience, New York, N.Y., 1959, pp.895-1005.
18. R. M. Noyes, J. Am. Chem. Soc., 81, 566 (1959); G. A. Salmon, and R. M. Noyes, ibid., 84, 672 (1962); S. A. Levison and R. M. Noyes, ibid., 86, 4525 (1964).
19. R. C. Reid and T. K. Sherwood, "The Properties of Gases and Liquids; Their Estimation and Correlation", 2nd ed., McGraw-Hill Book Co., New York, 1966.

20. E. G. Scheibel, Ind. Eng. Chem., 46, 2007 (1954).
21. C. R. Wilke and P. Chang, A. I. Ch. E. J., 1, 264 (1955);
C. R. Wilke, Chem. Eng. Progr., 45, 218 (1949).
22. A. Einstein, Ann. Physik., 17, 549 (1905).
23. A. M. North, Quart. Rev. (London), 20, 421 (1966).
24. Ibid., "The Collision Theory of Chemical Reactions in Liquids", Methuen & Co., Ltd., London, 1964.
25. R. M. Noyes, Progr. Reaction Kinetics, 1, 130 (1961).
26. Ibid., J. Am. Chem. Soc., 86, 4529 (1964).
27. M. V. Smoluchowski, Z. physik. Chem., 92, 129 (1917).
28. F. C. Collins, J. Colloid. Sci., 5, 499 (1950).
29. E. C. Murray and R. N. Keller, J. Org. Chem., 34, 2234 (1969).
30. W. G. Herkstroeter and G. S. Hammond, J. Am. Chem. Soc., 88, 4769 (1966); W. G. Herkstroeter, Ph.D. Thesis, California Institute of Technology, 1965.
31. J. Hartmann, Astrophys. J., 8, 218 (1898).
32. See for example, E. B. Wilson, Jr., "An Introduction to Scientific Research", McGraw-Hill Book Co., New York, 1952, p. 219.
33. See for example, O. Dobis, J. M. Pearson, and M. Szwarc, J. Am. Chem. Soc., 90, 278 (1968).
34. F. D. Rossini et al., "Selected Values of Physical and Thermodynamic Properties of Hydrocarbons and Related Compounds", American Petroleum Institute Research Project 44, Carnegie Press, Pittsburg, Pa., 1953.

35. H. Tschamler, F. Wettig, and E. Richter, Mh. Chem., 80, 572 (1949).
36. J. H. Gorrell and J. T. Dubois, Trans. Faraday Soc., 63, 347 (1967).
37. A. Gierer and K. Wirtz, Z. Naturforschung, 8a, 532 (1953).
38. R. D. Burkhart, J. Phys. Chem., 73, 2703 (1969).
39. A. Beckett, A. D. Osborne, and G. Porter, Trans. Faraday Soc., 60, 873 (1964).